Mineral exploration with natural-source EM: comparing ground and airborne methods

Alan G. Jones
ManoTick GeoSolutions Ltd.
(alan.jones@manotick-geosolutions.com)

Seyed Masoud Ansari (Geological Survey of Canada)

Randall Mackie & Wolfgang Soyer (Viridien)

Presented at NSG 2025

VIRIDIEN

Natural Resources Canada

Ressources naturelles Canada

The problem…

We have to find **hundreds** of new deposits of all sorts of metals and minerals and bring them into active mining within the next decade or our technological advance will be throttled and we will not meet NetZero 2050 targets!

For example for Copper alone:

Current world production: **21 Mt**

Needed world production by 2050: **35 – 50 Mt**

200 major Cu mines will close by 2035 + Cu grades decreasing

➔ World production by 2035 estimate at **15 Mt**

➔ Need to find 200+ new deposits immediately and bring to mine

Overarching geophysical problem…

Ground-based deep-probing geophysical methods are too slow and expensive for the task at hand.

Need rapid coverage of large areas using cost-effective technologies

➔ Natural-source airborne EM (NSAEM) methods can possibly satisfy this demand

(but only if the EM response from the deposit is in the frequency range of the airborne systems!)

Obvious Advantages of NSAEM

1. Rapid EM exploration over a large area quickly and for a reasonable cost
2. High ”site” density compared to land-based equivalents – e.g. for ZTEM (Legault et al., 2012), MobileMT (Prikhodko et al., 2024) and QAMT (Larnier et al. 2021) a measurement is computed every 10-20 m on flight lines typically 200 m apart compared to 500 m sites in high density AMT (70x more sites)
3. Use for deposit discovery, follow-up with ground-based methods for higher resolution characterization

MT - magnetotellurics

(Chave and Jones, 2012)

Local 2-horizontal component **E** and local 3-component **H**

Relate the fields by:

$$\begin{bmatrix} Ex \\ Ey \\ Hz \end{bmatrix} = \begin{bmatrix} Zxx\ Zxy \\ Zyx\ Zyy \\ Tzx\ Tzy \end{bmatrix} \begin{bmatrix} Hx \\ Hy \end{bmatrix}$$

$$\underline{\mathbf{E}} = \underline{\mathbf{Z}}\ \underline{\mathbf{H}} \qquad \&$$

$$Hz = Tzx\ Hx + Tzy\ Hy$$

24 freqs modelled: 7.5 kHz – 10 Hz (8/decade)

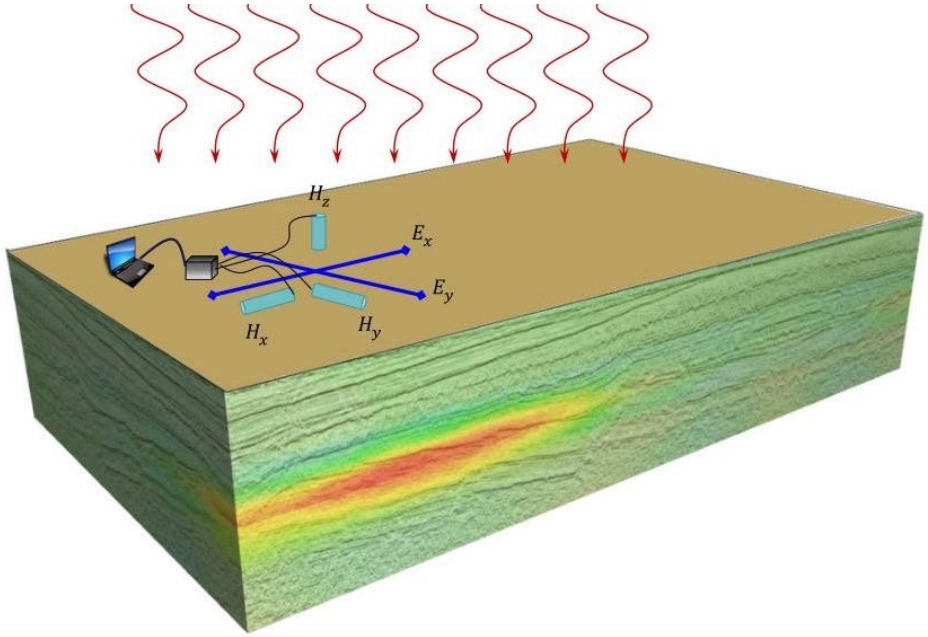

ZTEM – Z-Axis Tipper EM system

Helicopter-borne horizontal loop for Hz-air (Hza)

Two horizontal coils at a base station for Hx-base and Hy-base (Hxb & Hyb)

Measurements at six fixed frequencies:

30, 45, 90, 180, 360, and 720 Hz

Relate the fields by ZTEM Tippers ZT:

$$Hz_{air} = ZTzx\ Hx_{base} + ZTzy\ Hy_{base}$$

The conventional Tipper comes from "local" **H**:

$$Hz_{local} = Tzx\ Hx_{local} + Tzy\ Hy_{local}$$

(Dependence on frequency assumed)

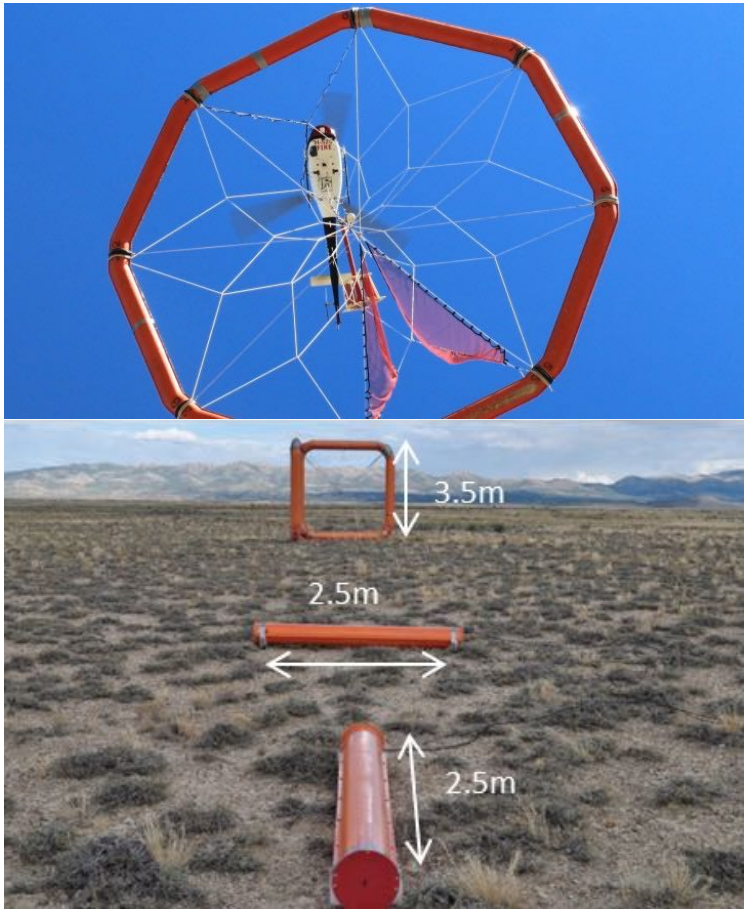

MobileMT

Helicopter-borne total component – no orientation information (from 3-component coils in a bird) for |H|-air

Electrode array at the base (Exb & Eyb)

Measurements at up to 30 frequencies from 25 Hz – 20 kHz, 9 pts/decade, but no AMT deadband

Various ways to compute apparent conductivity from the numerical fields derived by a modeling code. Here are four, and we use two of them:

1) Total |H| / Total |E| - which we use here for theoretical data generation

2) Sattel's method (only using 2 rows of the admittance tensor)

3) Cross-product of the admittance tensor – used in Viridien's code

4) Approximate determinant, such as Radić's

QAMT – Quantum AMT

Helicopter-borne fully-oriented mag fields (from LT squid in a bird) for **H**-air (Hxa, Hya, Hza)

Electrode array and 3-component mag at the base (Exb & Eyb; Hxb, Hyb, Hzb)

Estimates in the frequency range 25 Hz – 25 kHz (excluding AMT deadband)

Relate the fields by:

$$\underline{\mathbf{E}}_{base} = \underline{\mathbf{Z}}_{QAMT}\,\underline{\mathbf{H}}_{air} \qquad \& \qquad \underline{\mathbf{H}}_{air} = \underline{\mathbf{T}}_{QAMT}\,\underline{\mathbf{H}}_{base}$$

Also get **H**-gradient from: $\underline{\mathbf{\Delta H}} = \underline{\mathbf{H}}_{air} - \underline{\mathbf{H}}_{base}$

(but would need another base site for remote referencing)

➔ In final stages of development

Three theoretical natural source airborne systems

Three theoretical natural source airborne systems (AS) will be studied that bear similarities to systems currently in use – ZTEM, MobileMT and QAMT:

AS1: Airborne system 1: Only Hz measured in the air (Hza), and related to horizontal H fields (Hxb, Hyb) at the base station:

6 freqs – 800, 400, 200, 100, 50, 30 Hz

AS2: Airborne system 2: Measurement of all 3 components in the air (Hxa, Hya, Hza), but without orientation, and related to base station horizontal electric fields (Exb, Eyb):

14 freqs: 629, 500, 397, 315, 270, 199, 158,125, 99, 79, 63, 50, 39, 25 Hz

AS3: Airborne system 3: Measurement of all 3 components in the air (Hxa, Hya, Hza), with orientation, and related to base station horizontal electric (Exb, Eyb) and magnetic (Hxb, Hyb) fields – AS3 will not be discussed today

Lalor deposit, Snow Lake, northern Manotiba

The 14.4-Mt Lalor copper-zinc-gold deposit is situated in the Flin Flon Greenstone Belt of north-central Manitoba. It is large (>900 × 700 m) but deeply buried (>550 − 1200 m) deposit and was discovered using Crone-EM, a deep penetrating ground fixed-loop time-domain controlled-source EM system (EM) in 2007.

The Lalor deposit is wholly-owned and being mined by HudBay Minerals of Canada. It has been extensively studied by academic groups as part of a number of projects.

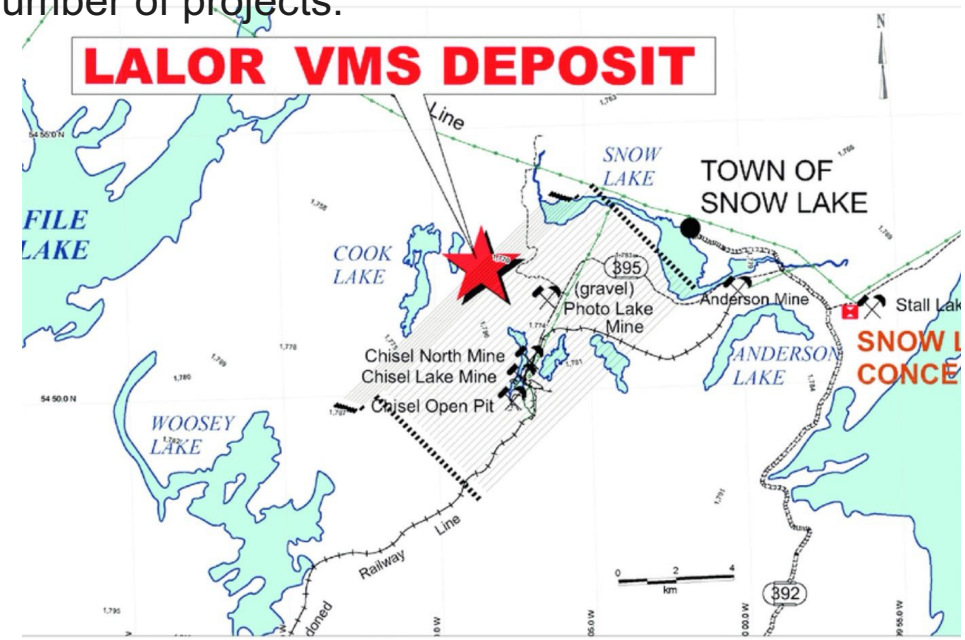

Lalor numerical model

The most detailed model of any deposit created to date – over 5 million cells

GEOPHYSICS, VOL. 85, NO. 5 (SEPTEMBER-OCTOBER 2020); P. E171–E190, 17 FIGS., 2 TABLES.
10.1190/GEO2019-0214.1

Three-dimensional magnetotelluric numerical simulation of realistic geologic models

SeyedMasoud Ansari[1], Ernst Schetselaar[1], James Craven[1], and Colin Farquharson[2]

Three-dimensional magnetotelluric modelling of the Lalor volcanogenic massive-sulfide deposit, Manitoba

S.M. Ansari[1*], E.M. Schetselaar[1], and J.A. Craven[1]

Ansari, S.M., Schetselaar, E.M., and Craven, J.A., 2022. Three-dimensional magnetotelluric modelling of the Lalor volcanogenic massive-sulfide deposit, Manitoba; in *Targeted Geoscience Initiative 5: volcanic- and sediment-hosted massive-sulfide deposit genesis and exploration methods, (ed.) J.M. Peter and M.G. Gadd; Geological Survey of Canada, Bulletin 617, p. 313–327. https://doi.org/10.4095/328003*

Geophys. J. Int. (2023) **233,** 1245–1270
Advance Access publication 2022 December 26
GJI Geomagnetism, Rock Magnetism and Palaeomagnetism

http

A fully finite-element based model-space algorithm for three-dimensional inversion of magnetotelluric data

S.M. Ansari and J.A. Craven
Geological Survey of Canada, Natural Resources Canada, 601 *Booth Street, Ottawa, Ontario, K*1*A*0*E*9*, Canada.*
E-mail: seyedmasoud.ansari@nrcan-rncan.gc.ca; jim.craven@nrcan-rncan.gc.ca

Lalor finite element model grid

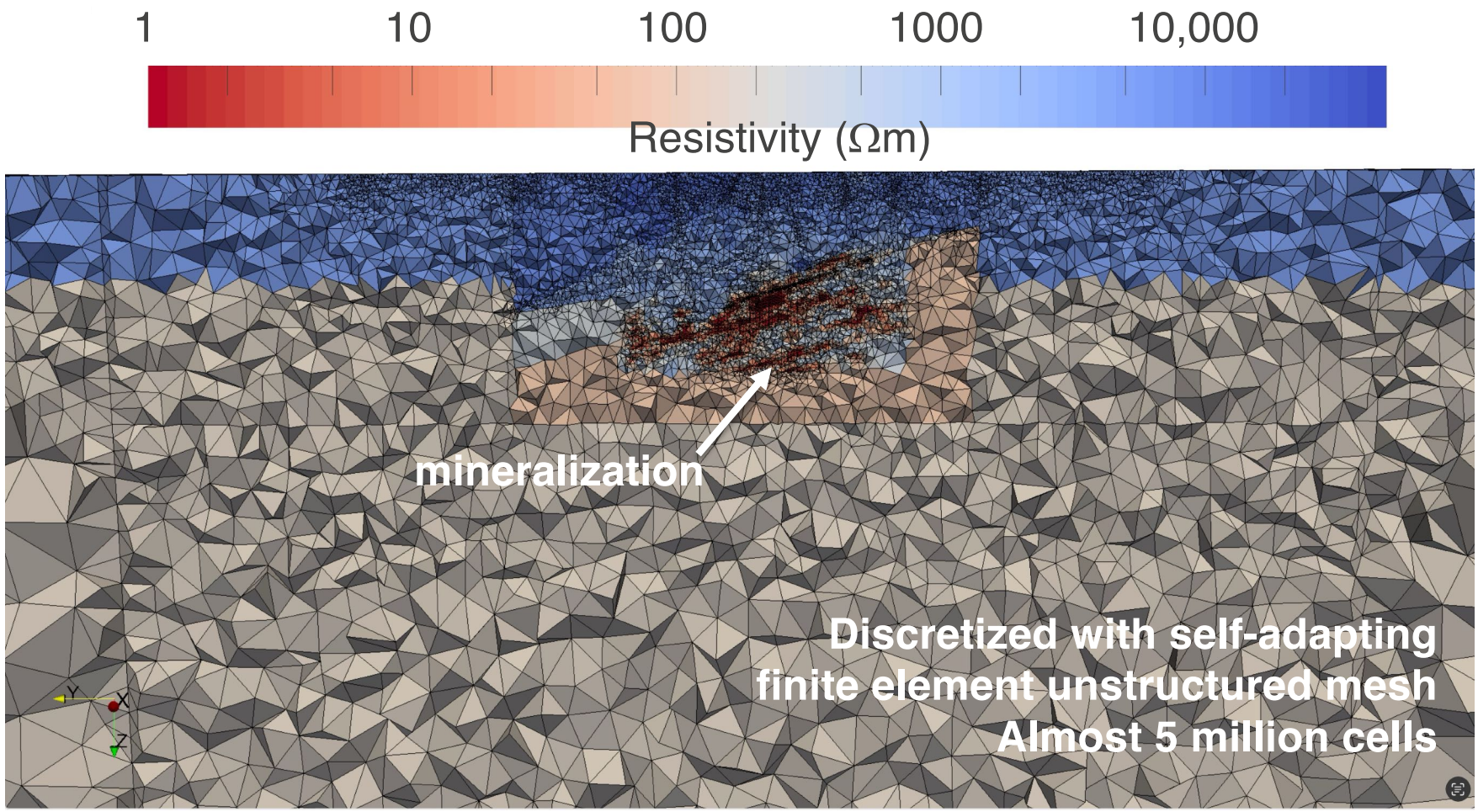

Lalor resistivity model – vertical slice

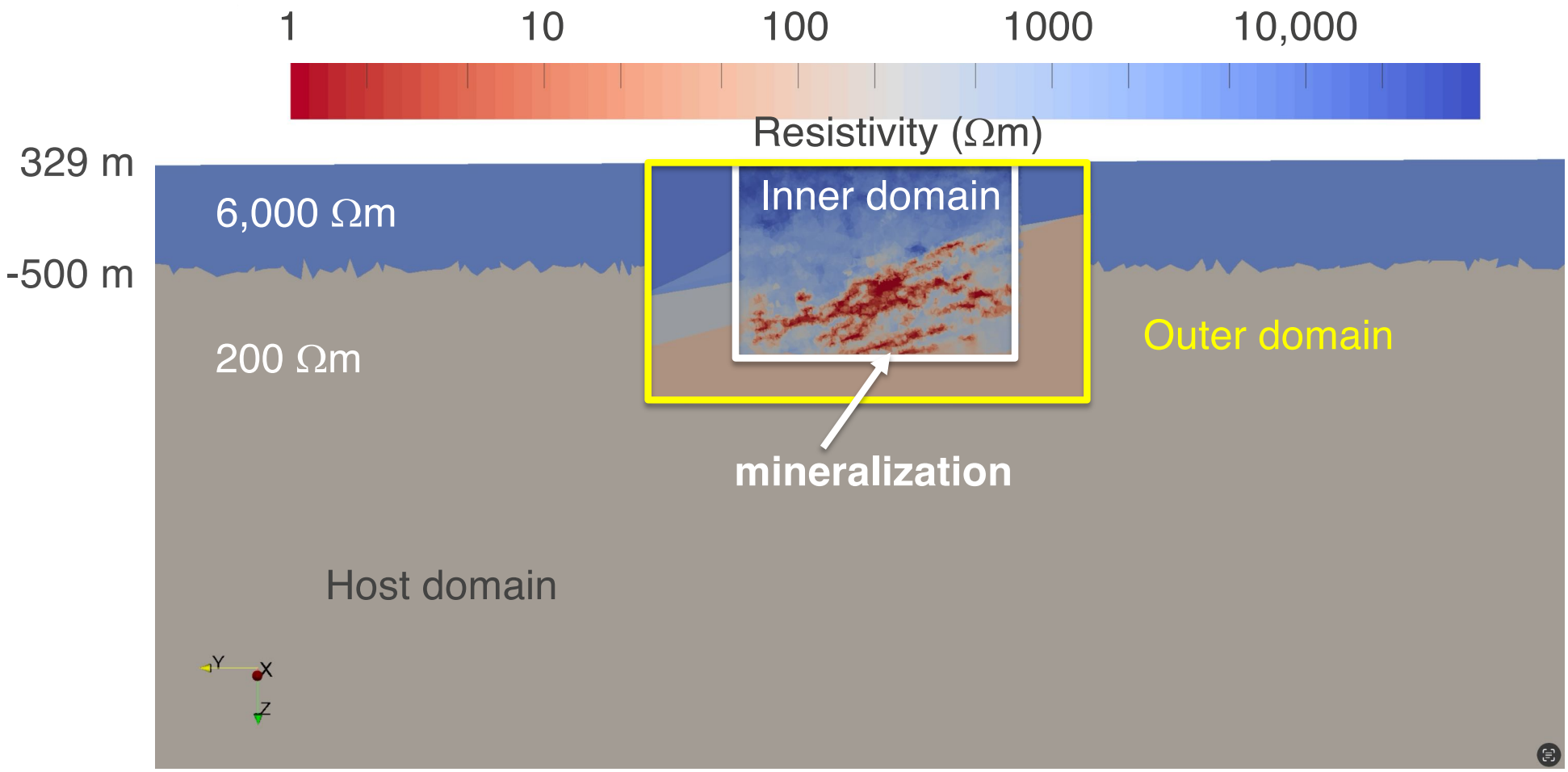

Lalor model depth slices:

200m
400m
700m
1100m

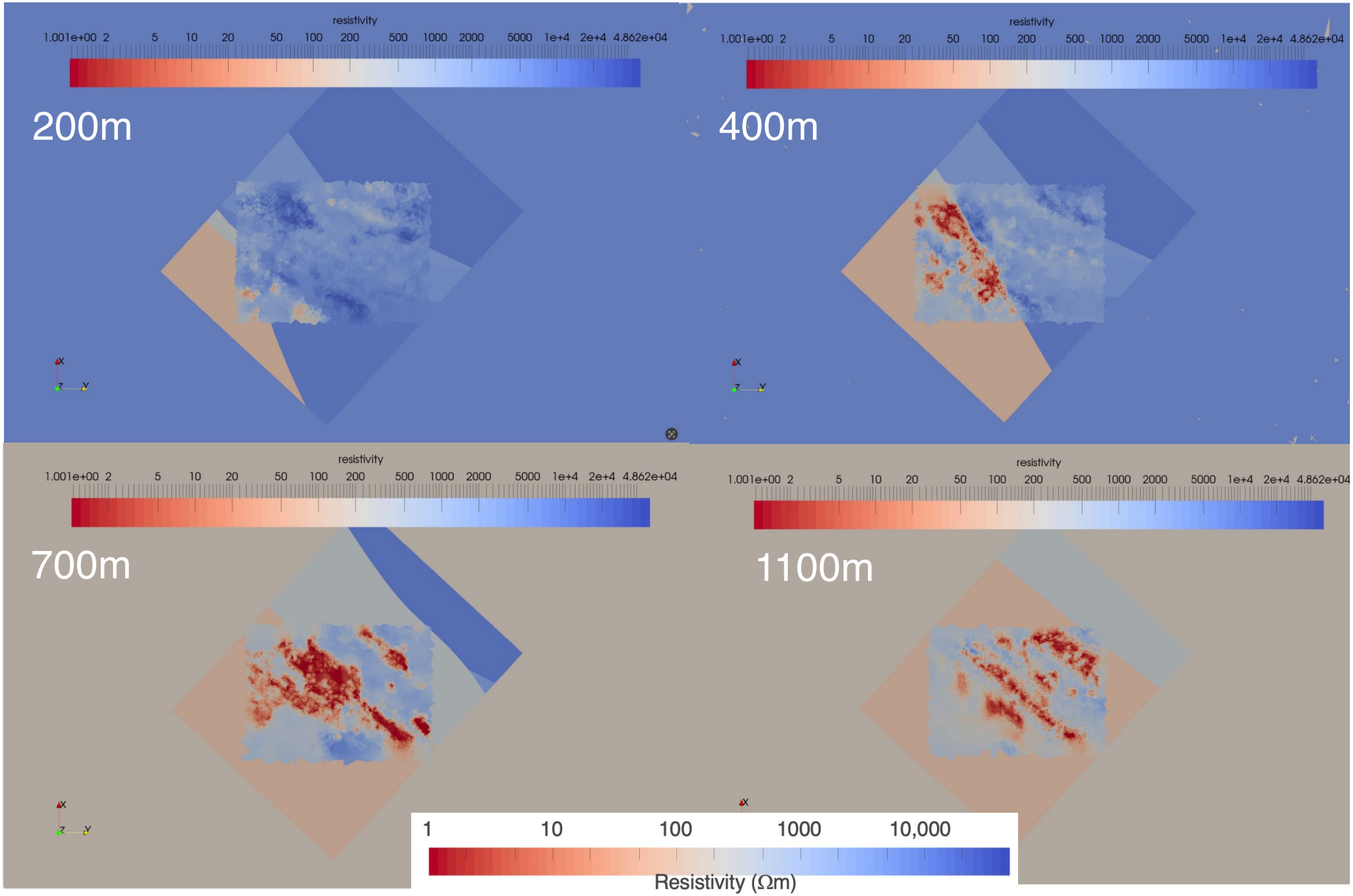

Anomalous fields at 200 Hz for a N-S e-source

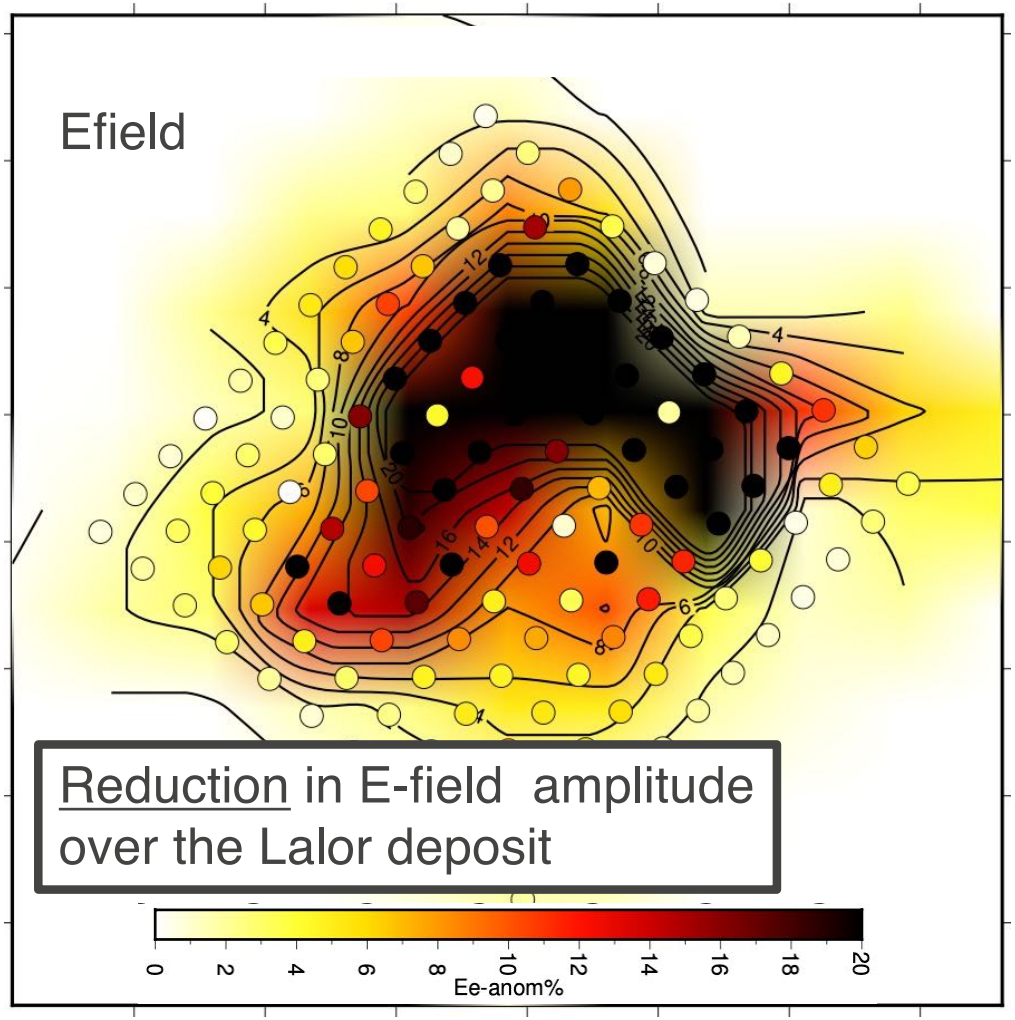

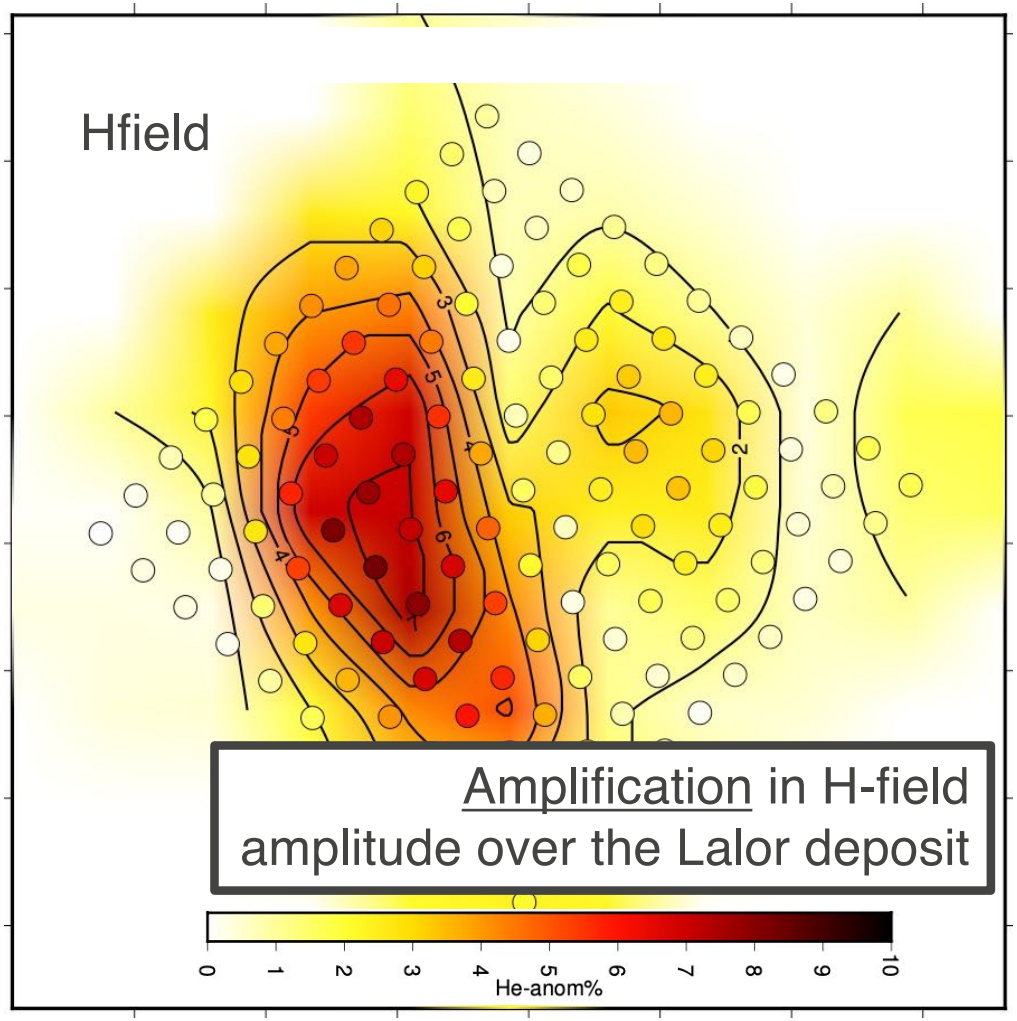

Anomalous fields at 200 Hz for a N-S e-source

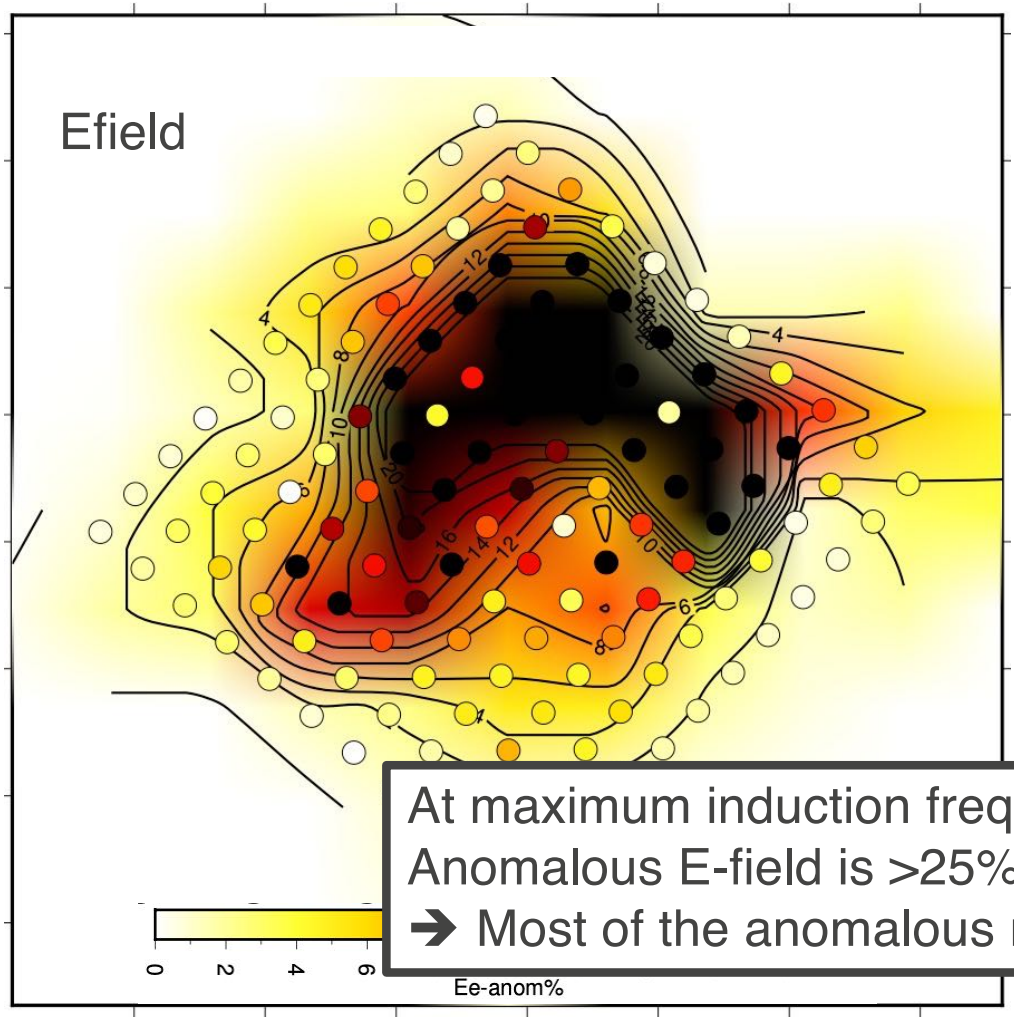

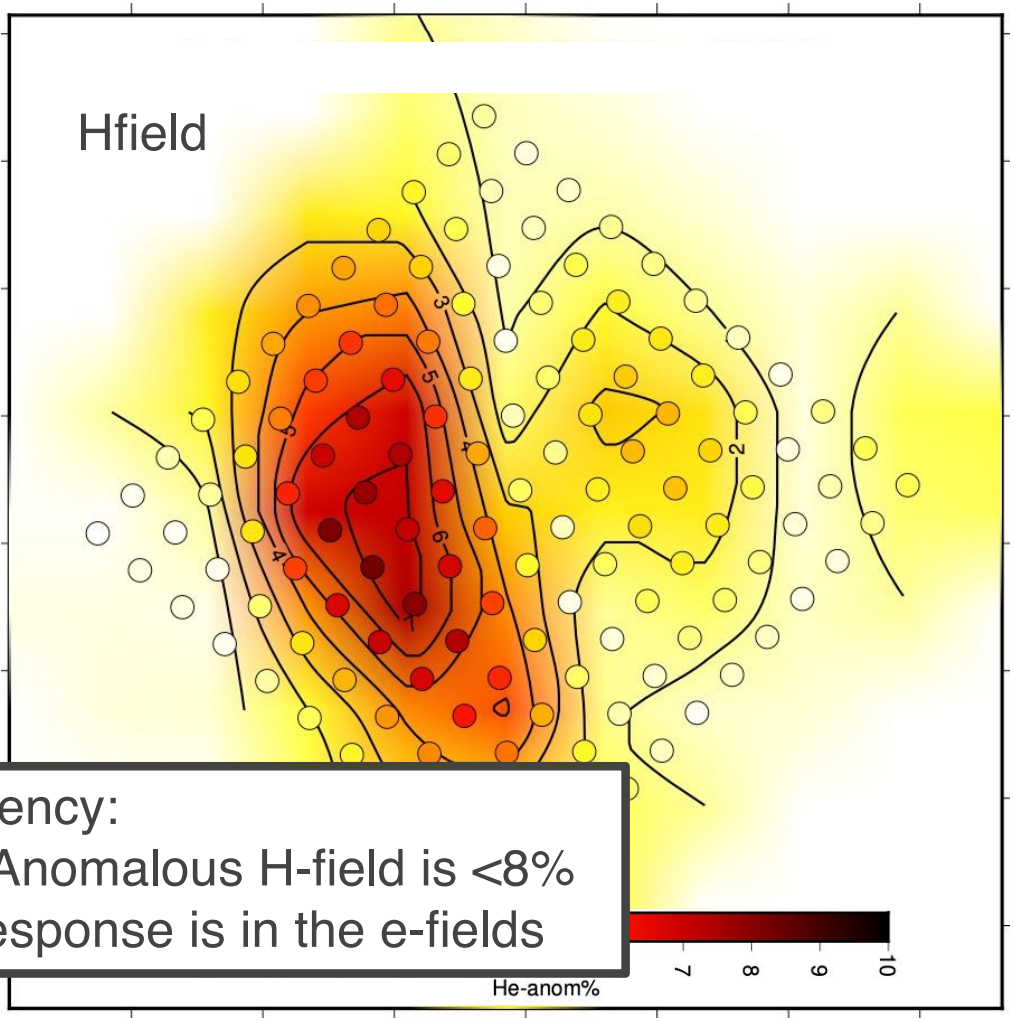

At maximum induction frequency:
Anomalous E-field is >25% Anomalous H-field is <8%
➔ Most of the anomalous response is in the e-fields

Lalor – MT Pha responses at 200 Hz

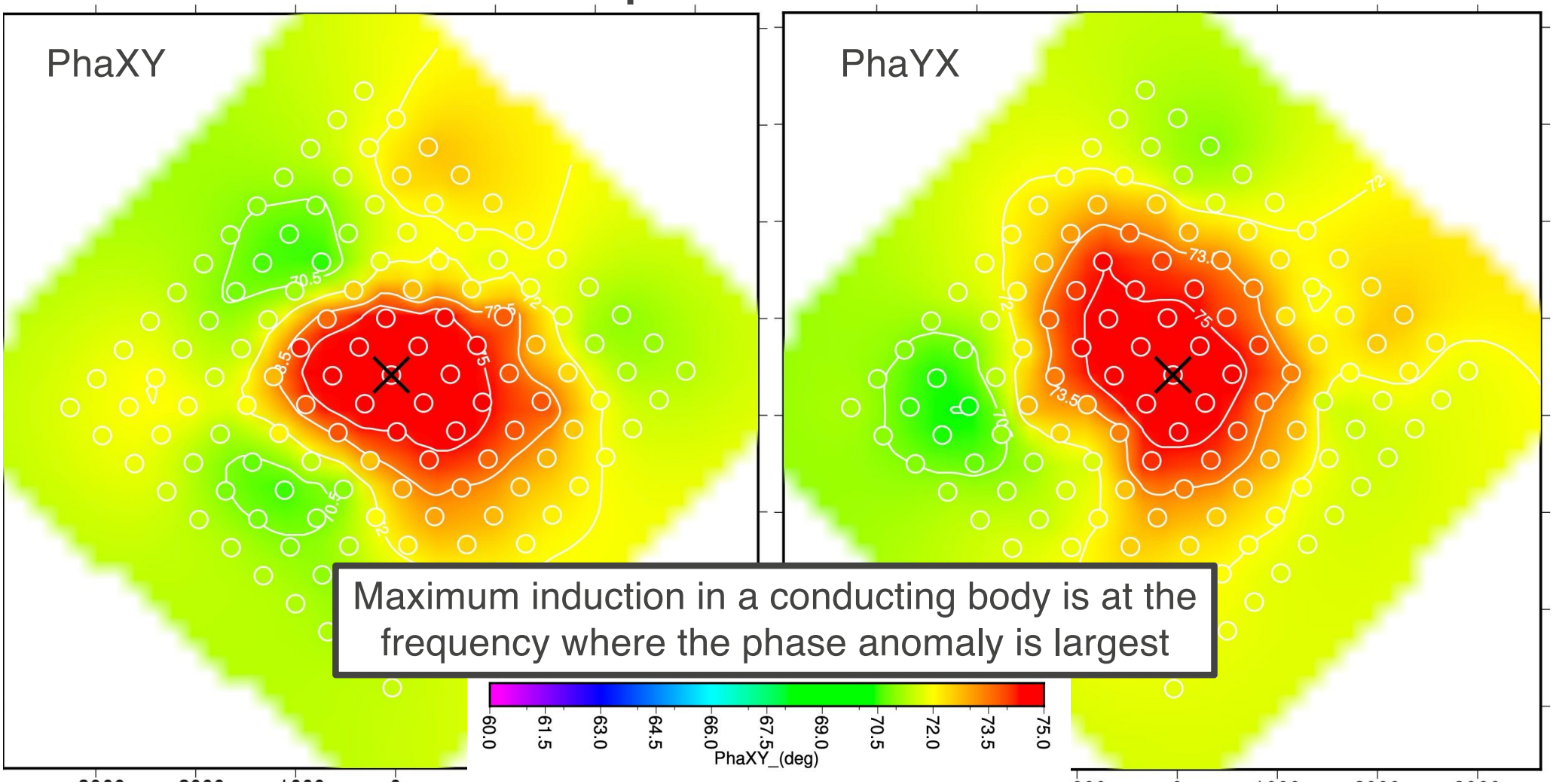

Maximum induction in a conducting body is at the frequency where the phase anomaly is largest

Lalor – MT Pha responses at 200 Hz

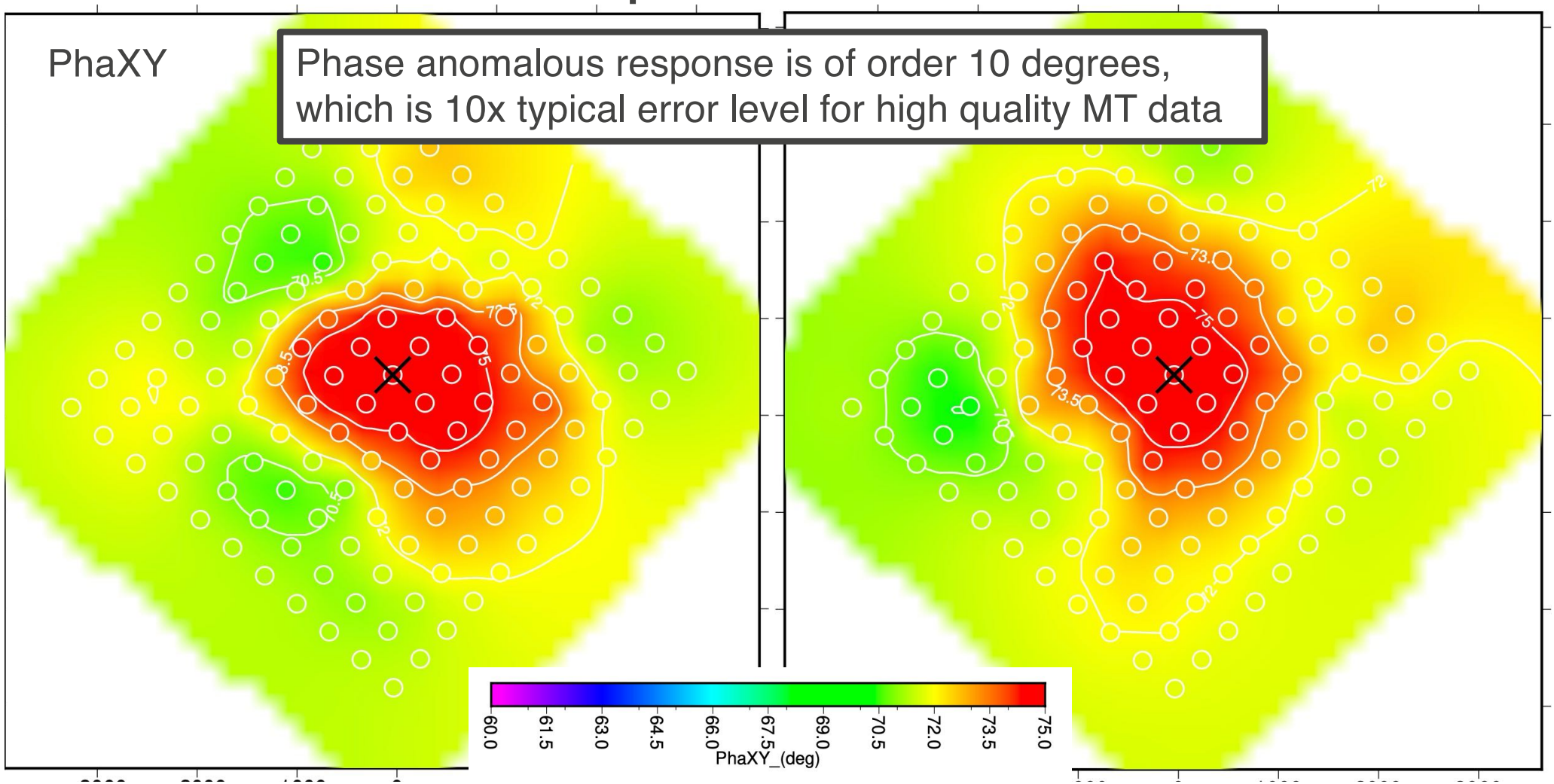

Lalor – Tipper magnitude responses at 200 Hz

|Tipperl response also maximises @ 200 Hz of order 0.075

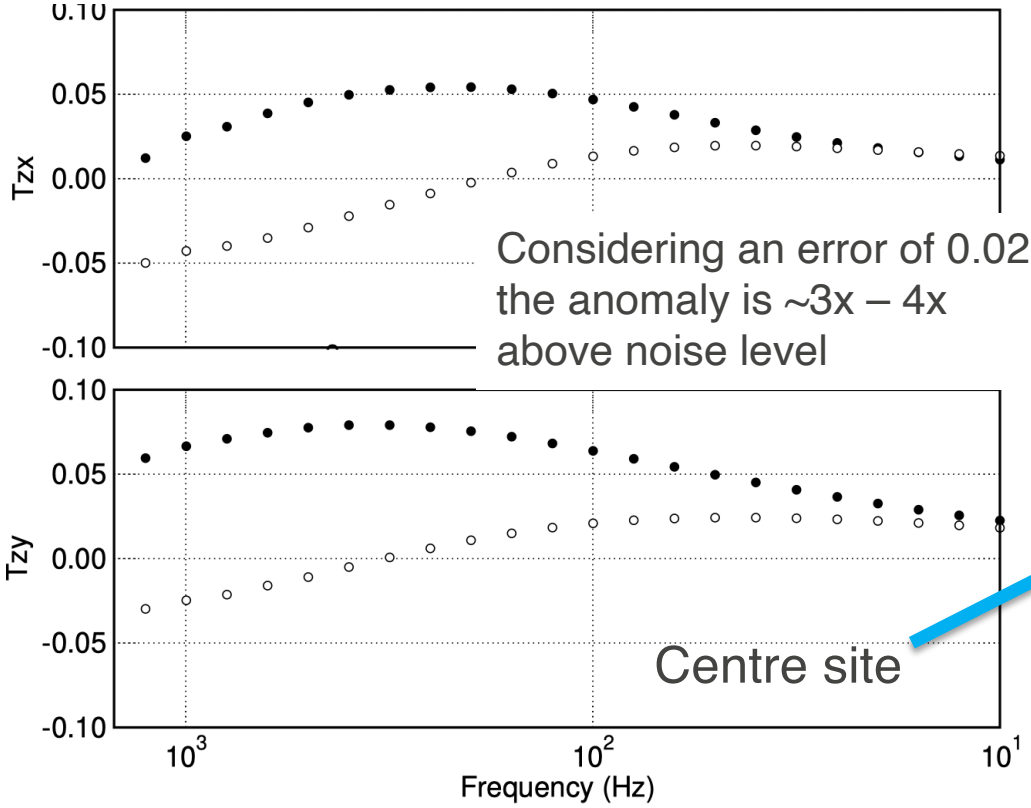

Considering an error of 0.02, the anomaly is ~3x – 4x above noise level

Centre site

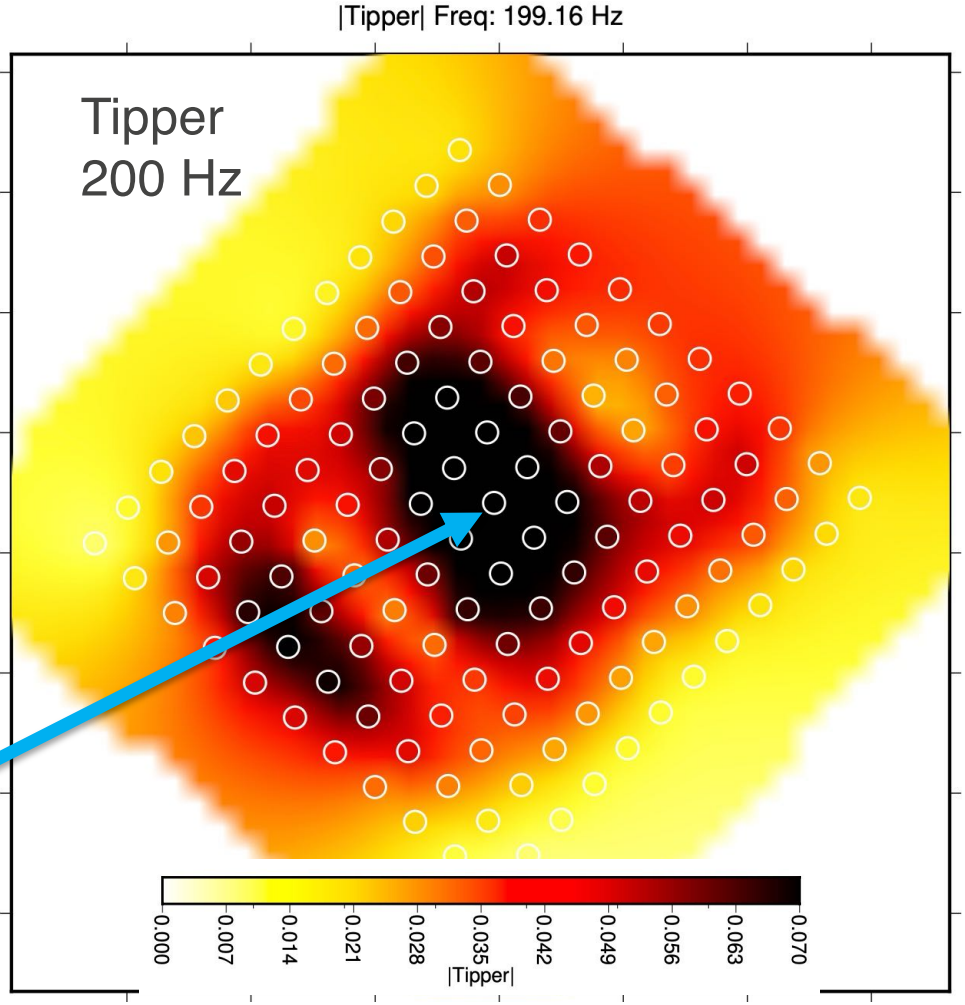

Lalor – Airborne System 1 responses at 180 Hz

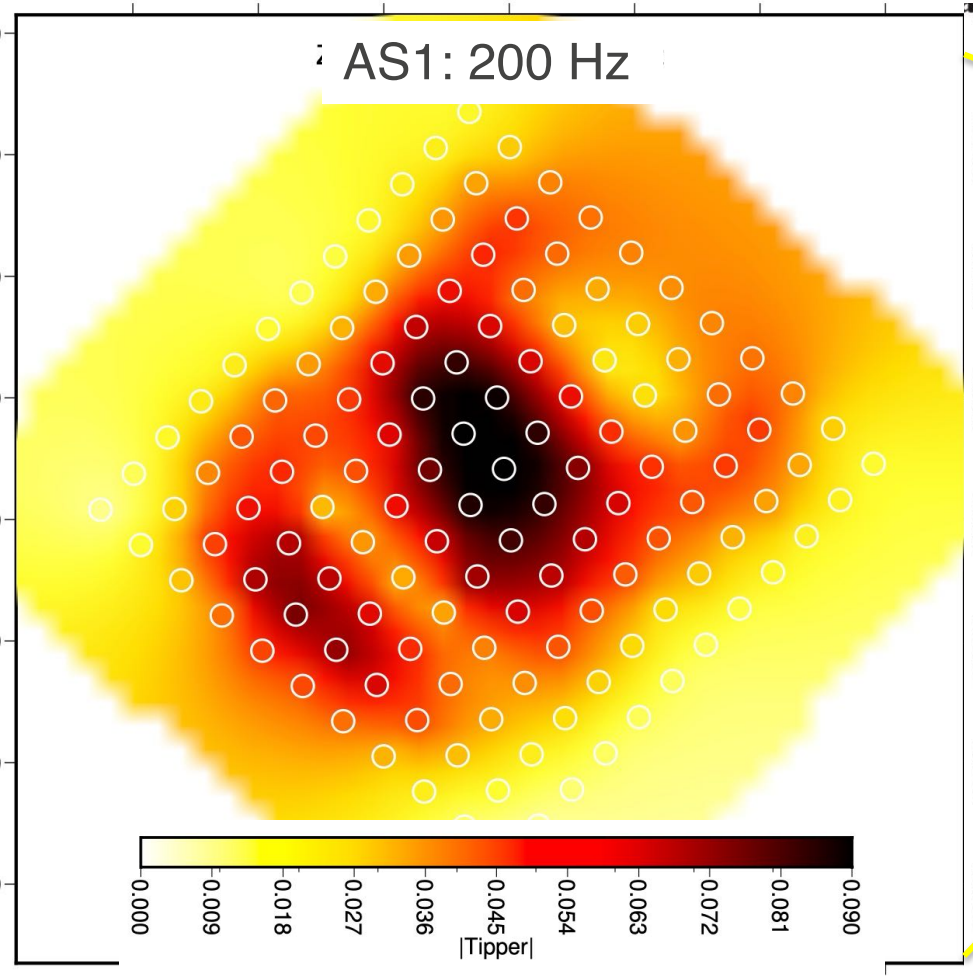

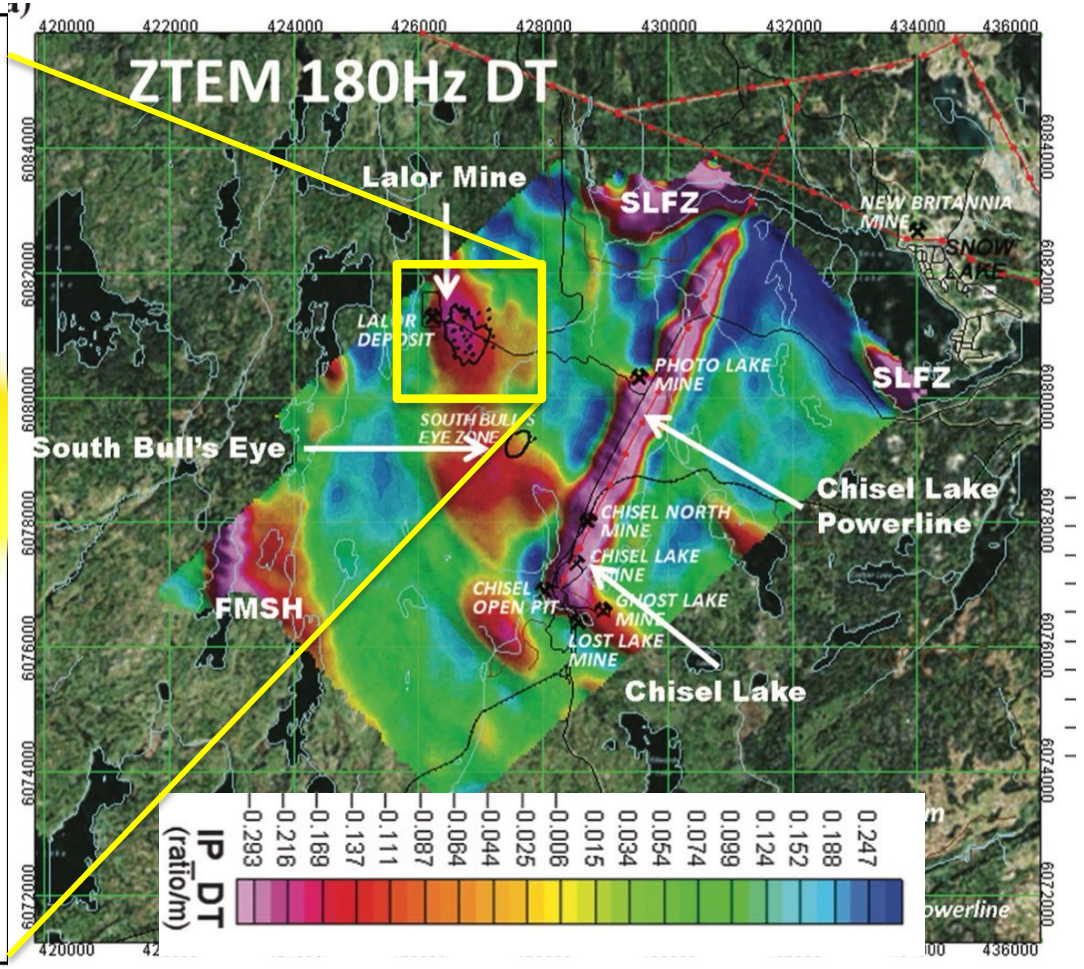

Lalor – Airborne System 2 responses at 200 Hz

AS2 maximum anomaly response @ 200 Hz is of order 0.68 mS/m (1,470 Ωm), compared to the background of 0.615 mS/m (1,626 Ωm)
➔ 9.5% anomaly in RhoA

Considering an error level of 3%-4%, the anomaly is ~2x – 3x above noise level

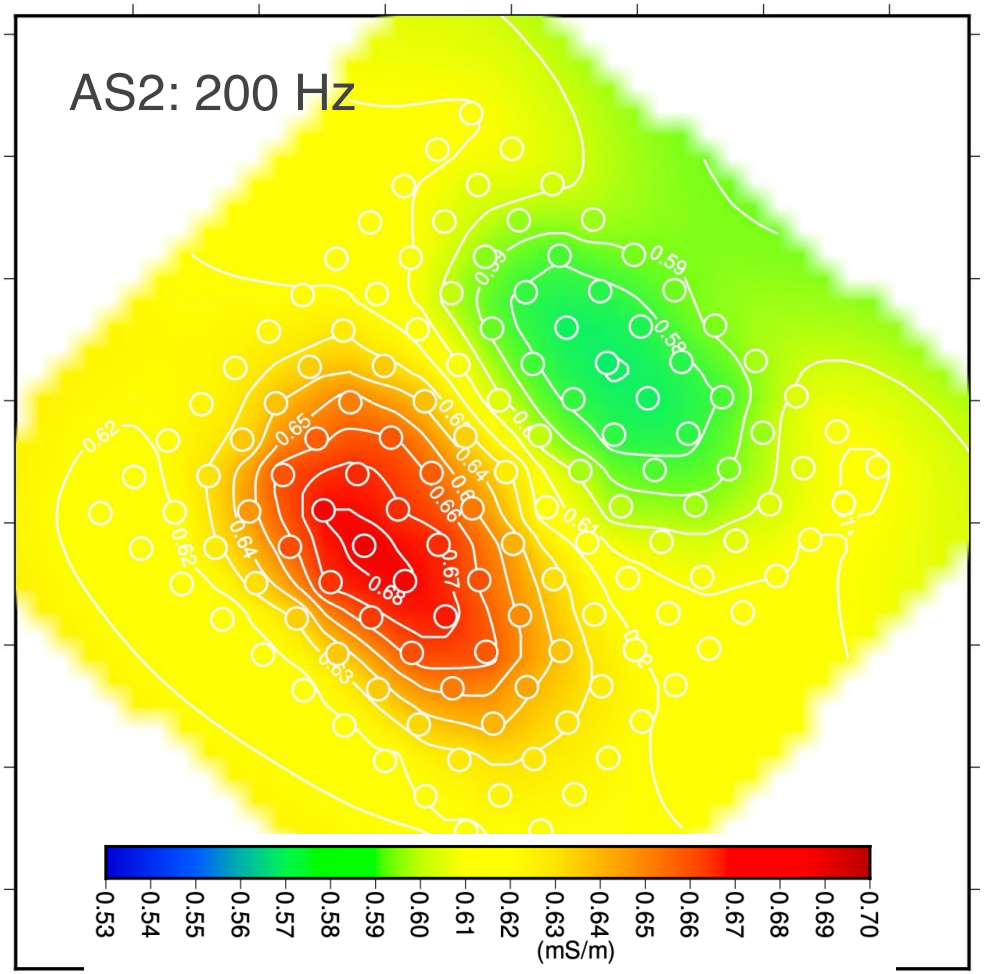

Lalor – ground MT compared to AS2 at 250 Hz

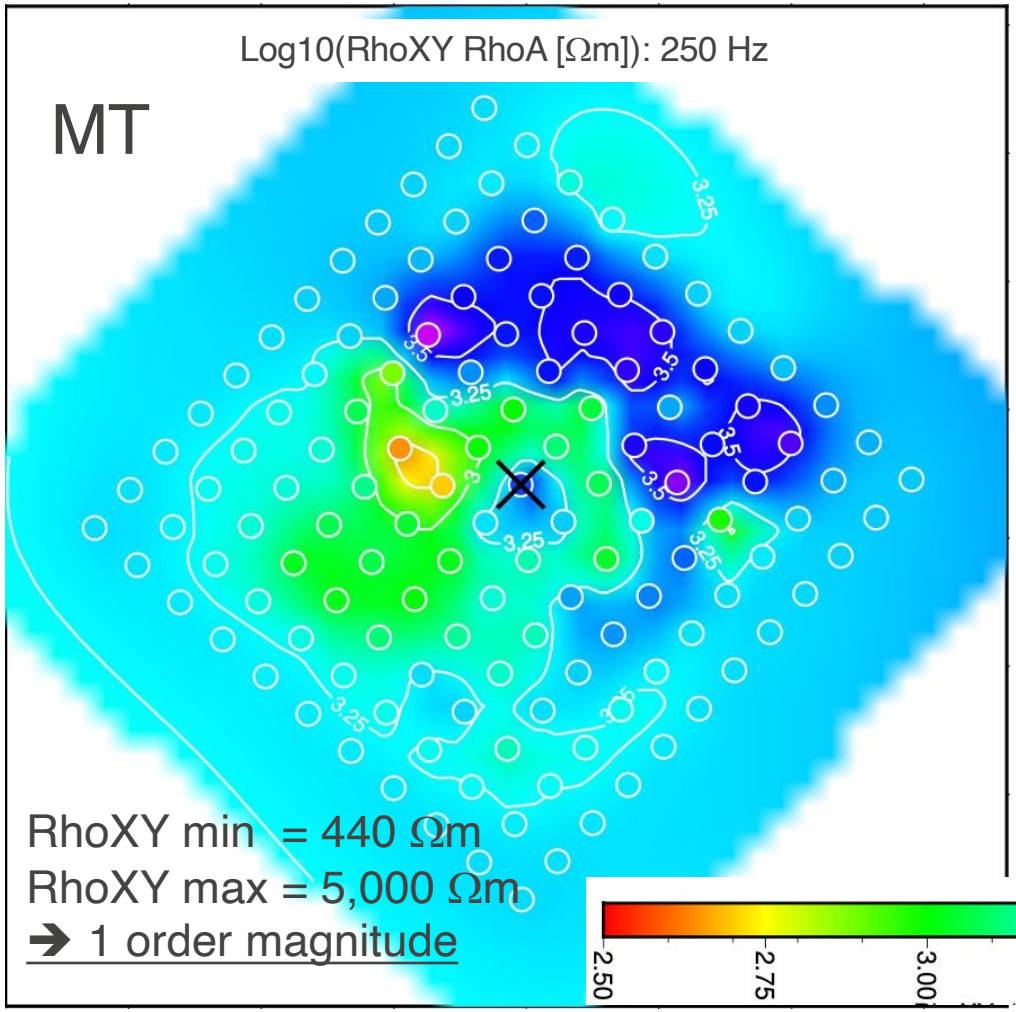

RhoXY min = 440 Ωm
RhoXY max = 5,000 Ωm
➔ 1 order magnitude

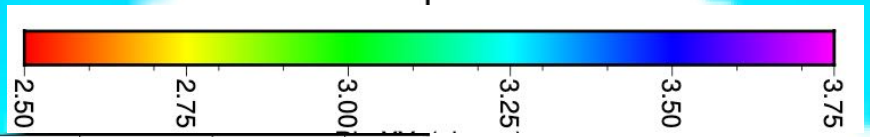

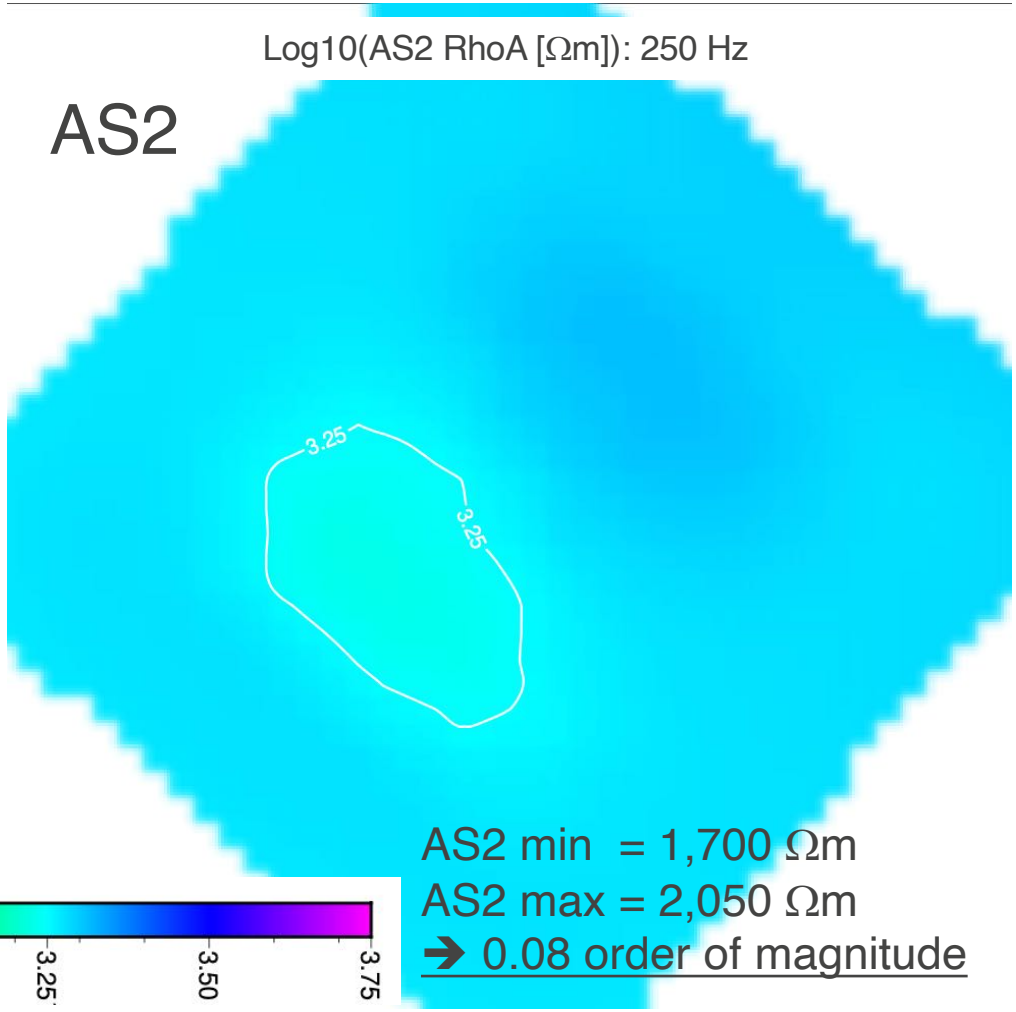

AS2 min = 1,700 Ωm
AS2 max = 2,050 Ωm
➔ 0.08 order of magnitude

Inversions – MT in 3-D using RLM-3D

RLM-3D is a general EM 3D inversion code by Randy Mackie (Viridien).

Uses rectilinear cells.

➔ Note that we are using a <u>different</u> forward solver to create the data (FE) than to invert the data (FD)!

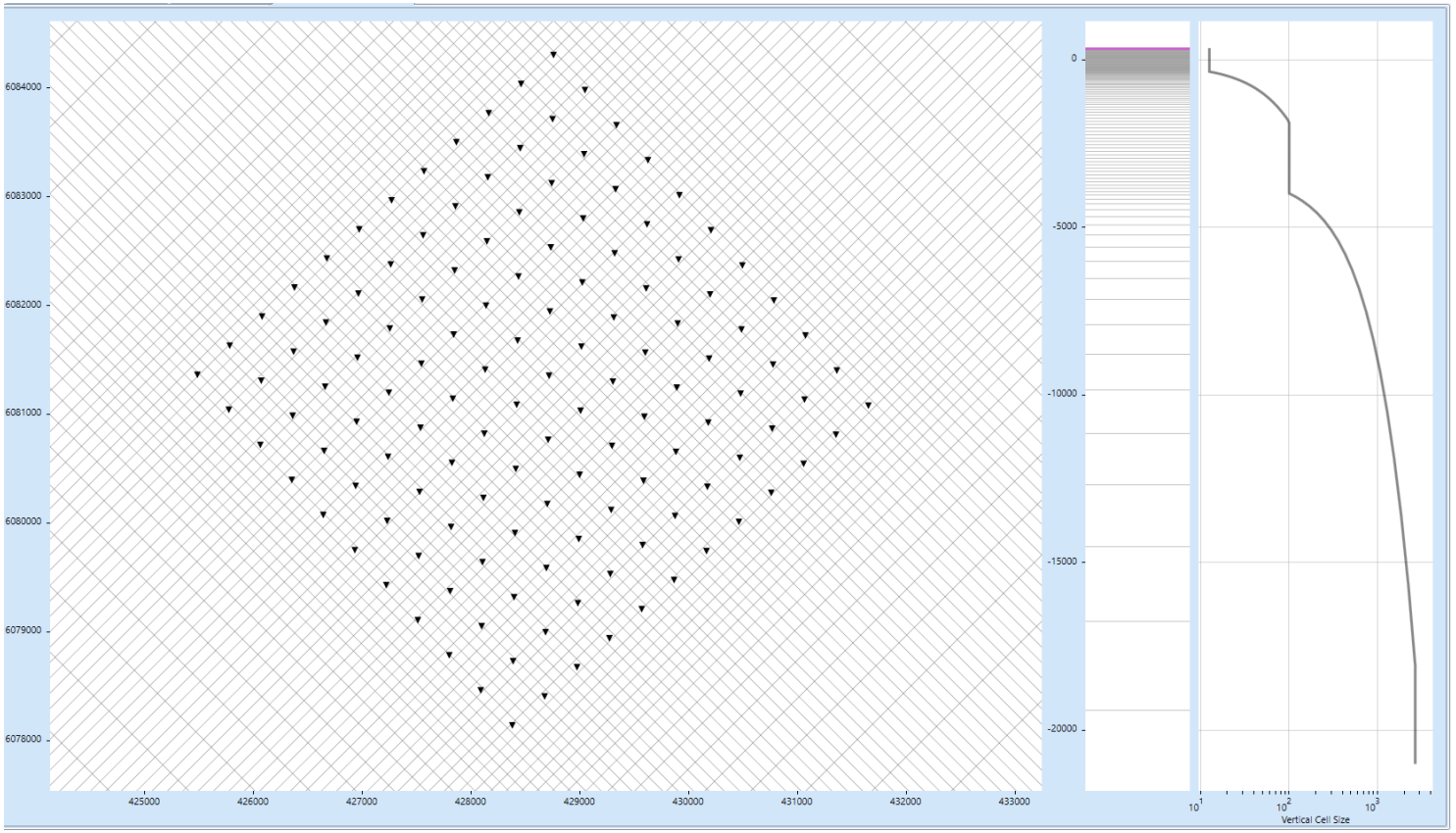

1.25M cells
100m x 100m x 12.5m in core

Model presentations

Going to show inverted models compared with the true model.

Shown for the true model is the 2 Ωm mineralization in black, and one NW-SE slice through the true model

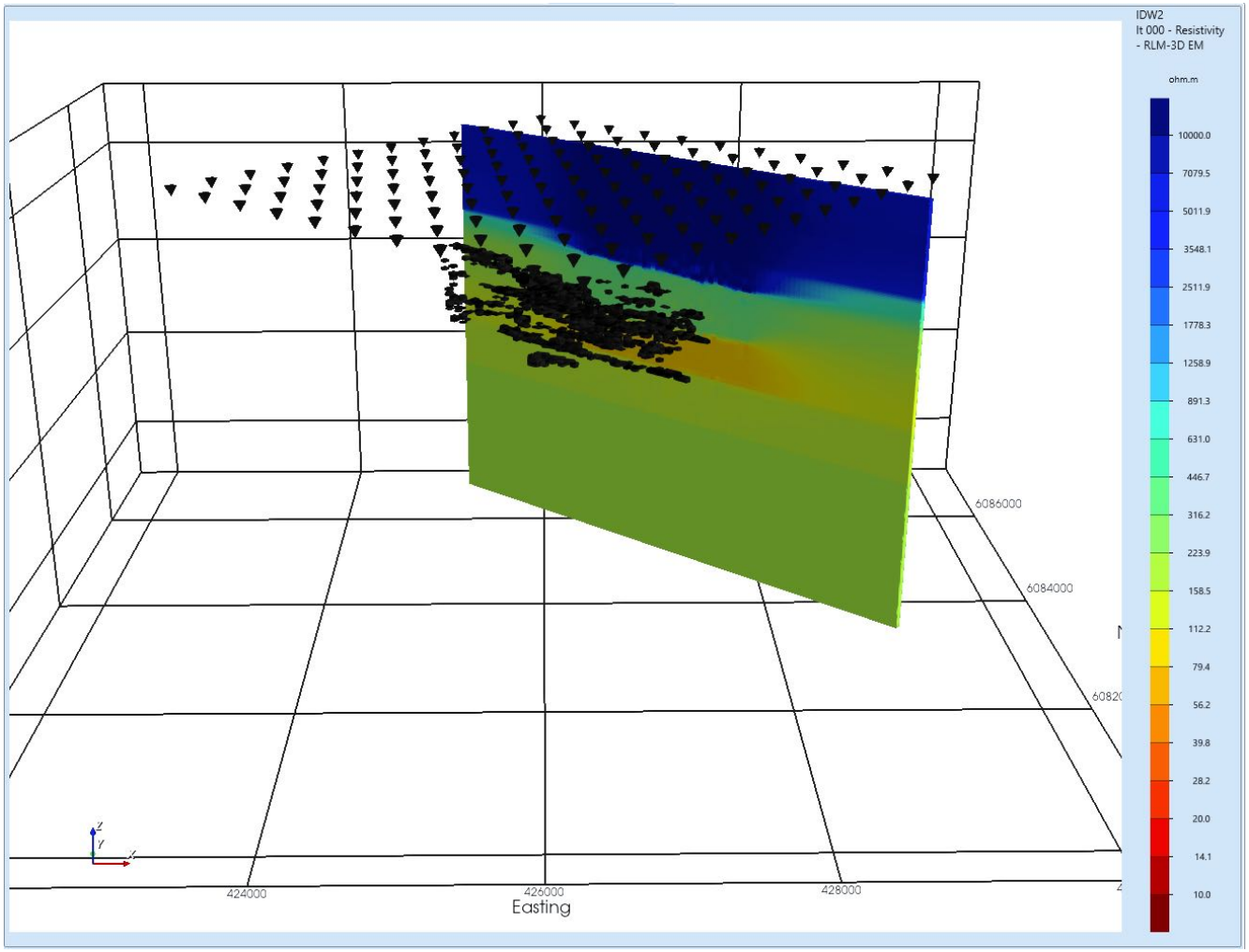

Inversions – MT in 3-D using RLM-3D

Final MT model

Outline of 50 Ωm surface and 20 Ωm central core very well defines the location of the mineralized zone 2 Ωm (black)

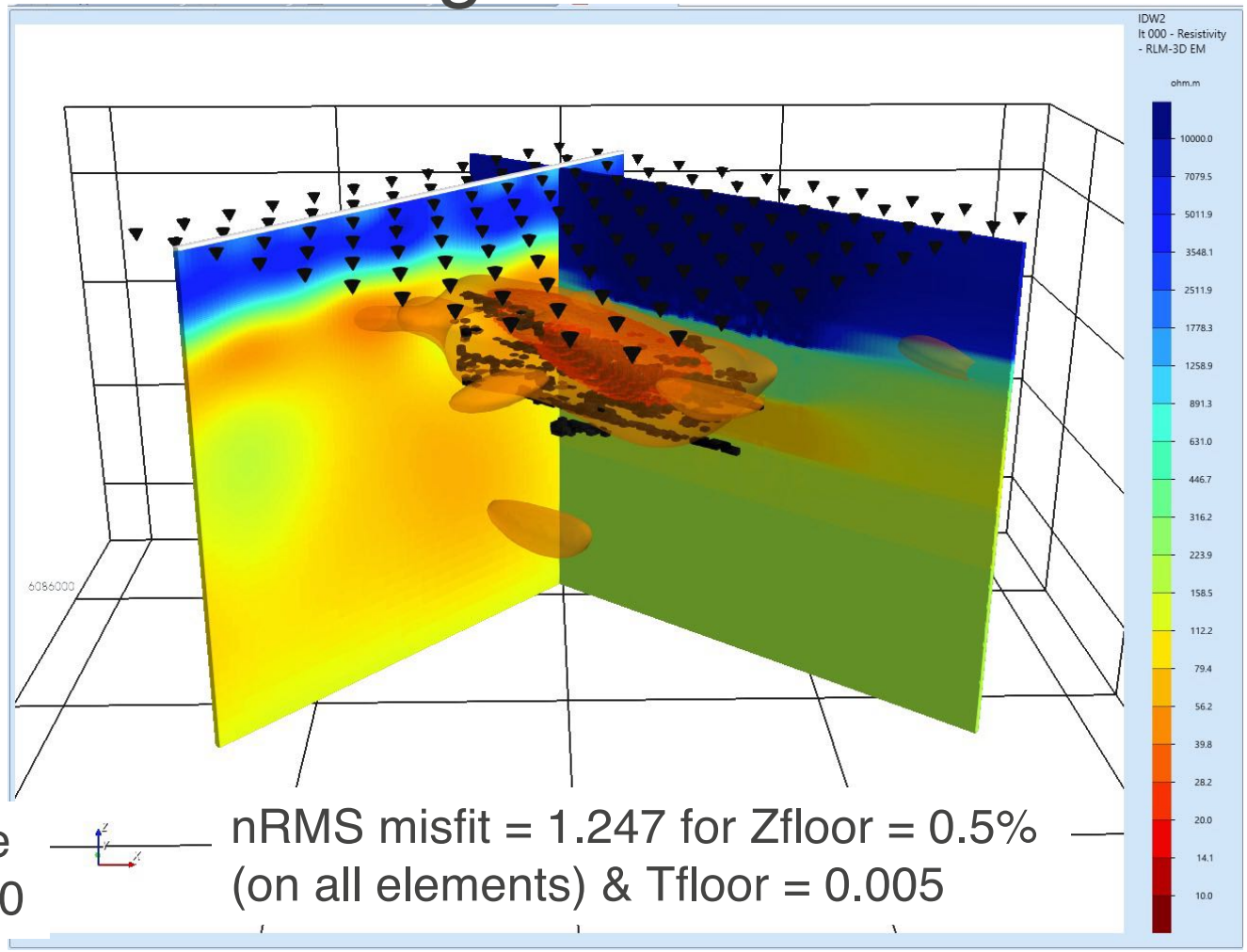

Start model: 200 Ωm half-space
RMS misfit to Start model: 58.90

Run AS1 – Model Iter50

Start model: 200 Ωm half-space

Misfit to half-space is **1.116**!

Iter50 (RMS=0.184) a body of Rho=60 Ωm below the mineralization and 100 Ωm surface is even deeper and more laterally extensive
➔ Lowest freq 30 Hz not yet through the bottom of the body

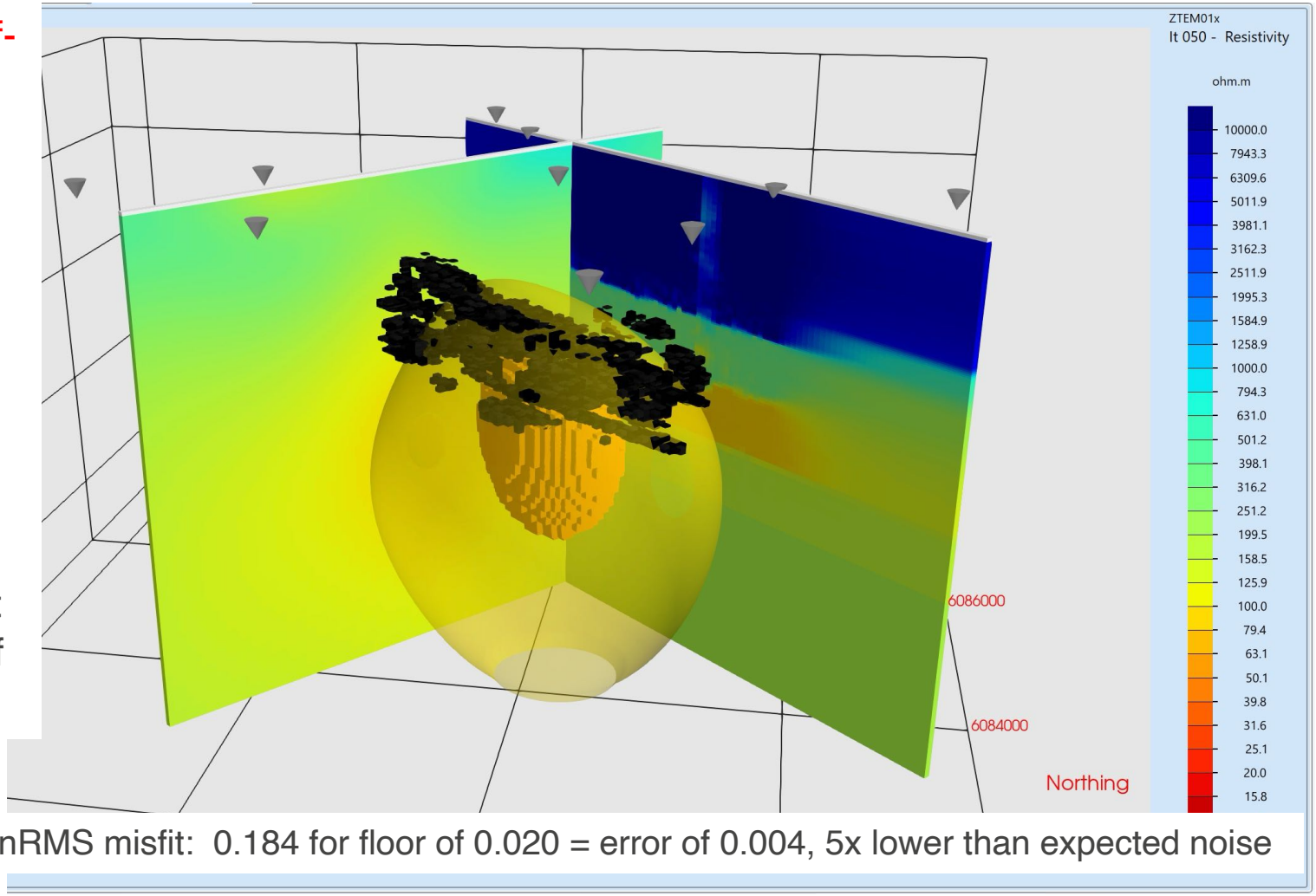

nRMS misfit: 0.184 for floor of 0.020 = error of 0.004, 5x lower than expected noise

Inversions – AS2 in 3-D using RLM-3D

AS2 data inversion relatively in its infancy cf. our knowledge of MT inversion.

Start model: 200 Ωm half-space

RMS misfit to Start model: **1.075**

After 50 iterations images a conductor shallower than the true mineralization, and resistivity is of order 125 Ωm rather than 2 Ωm

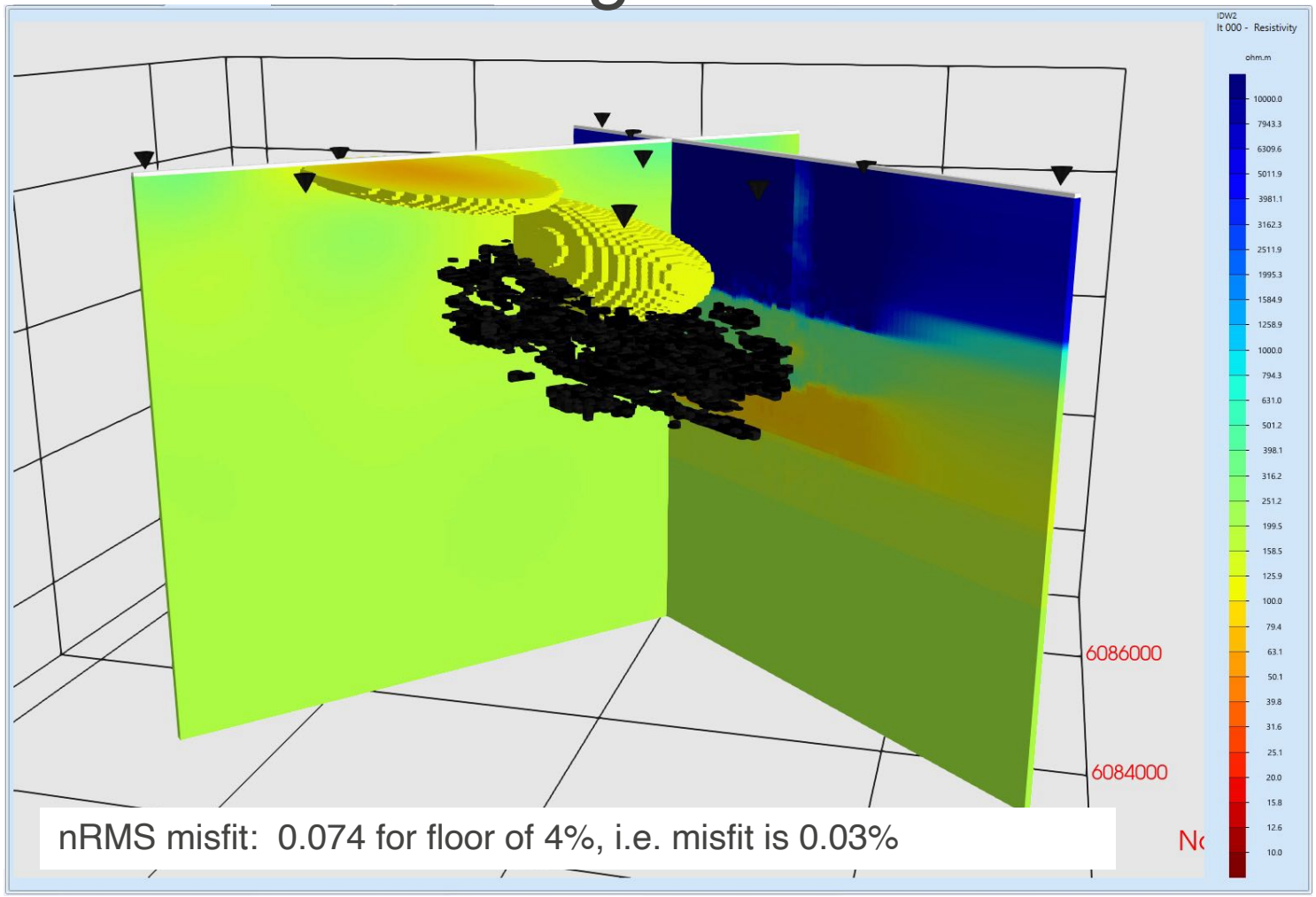

Inversions – AS2 in 3-D using RLM-3D

AS2 data inversion relatively in its infancy cf. our knowledge of MT inversion.

Start model: 2,000 Ωm half-space

After 50 iterations images a conductor at the depth of the true mineralization, but resistivity is of order 500 Ωm rather than 2 Ωm.

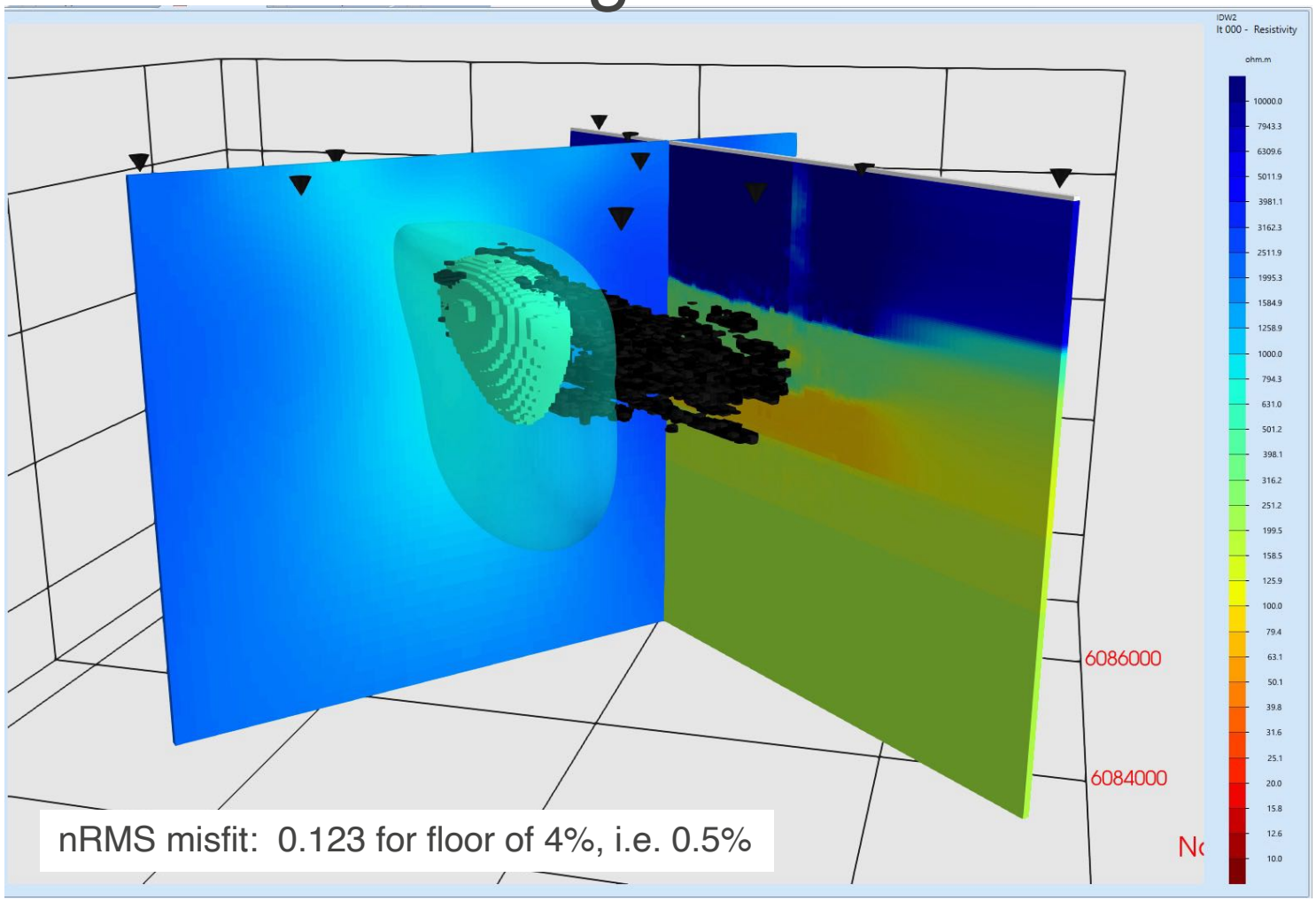

Inversions – AS2 in 3-D using RLM-3D

AS2 data inversion relatively in its infancy cf. our knowledge of MT inversion.

Start model: Smoothed Layered Earth – 6,000 Ωm over 200 Ωm

Very well images the conductor at the right depth, with a central core of 30 Ωm and a shell of 100 Ωm

➔ Knowledge of background critical

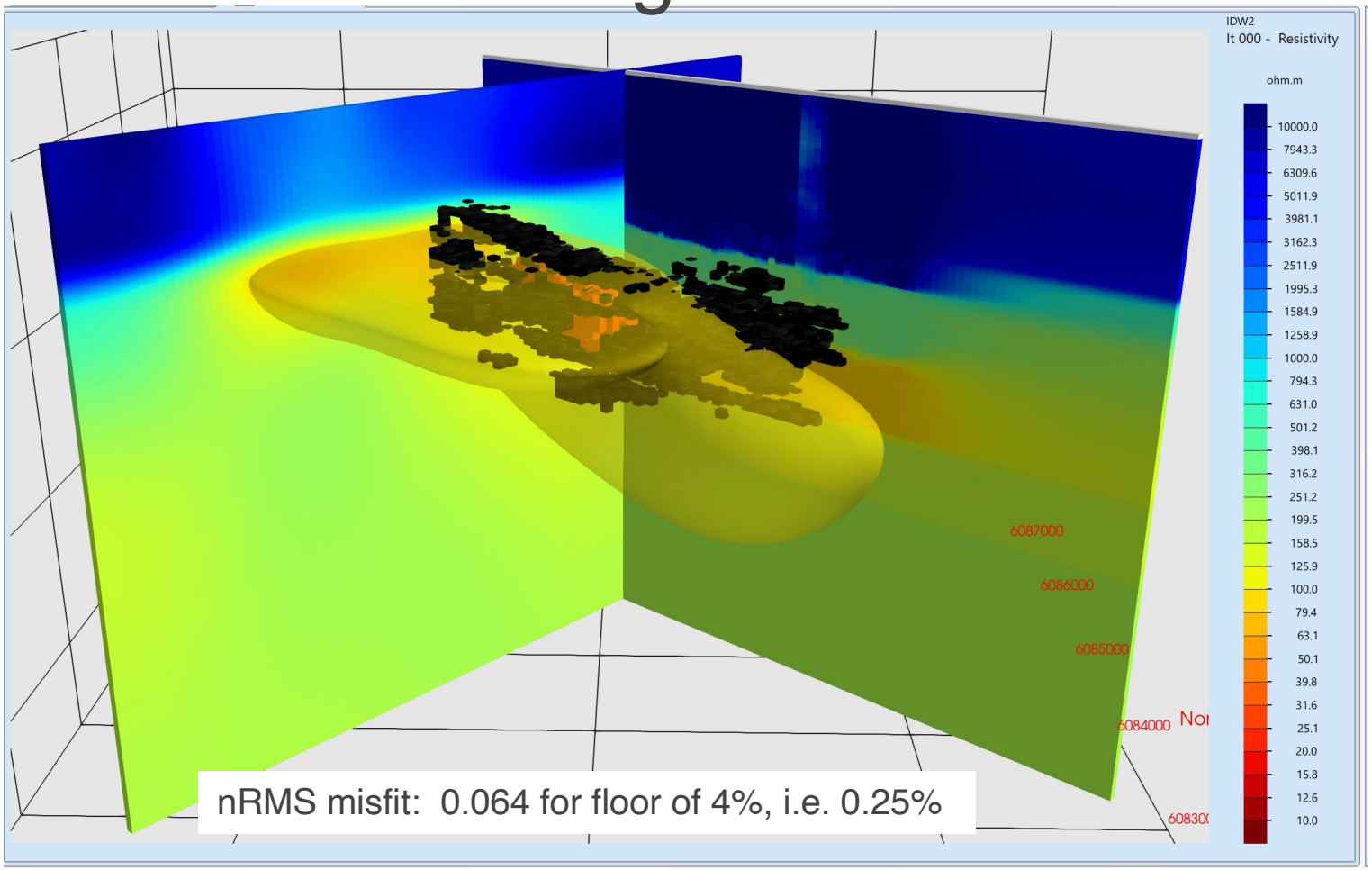

MT+AS1 & MT+AS2 inversion

1. Mimic a field campaign with ten sparse MT sites and full AS1 or AS2 coverage to see if adding in a few MT sites significantly improves resolution of the subsurface

2. Chose ten (10) sites randomly using ChatGPT:
   (Question posed: "*On a grid of 12 by 11 locations, pick ten locations randomly that are approximately equally spaced*")
   Site (x,y) pairs: (9,3), (4,7), (1,3), (10,0), (1,9), (7,9), (4,2), (11,8), (8,6), (0,0)
   Sites (12x+y+1): 112, 56, 16, 120, 22, 94, 50, 142, 103, 1

MT sites

Ten MT sites picked randomly within the grid and plotted on the inversion mesh

Note: This replicates poor terrane access.

Would be better to place the MT sites after the airborne survey at locations optimally chosen to improve resolution the greatest

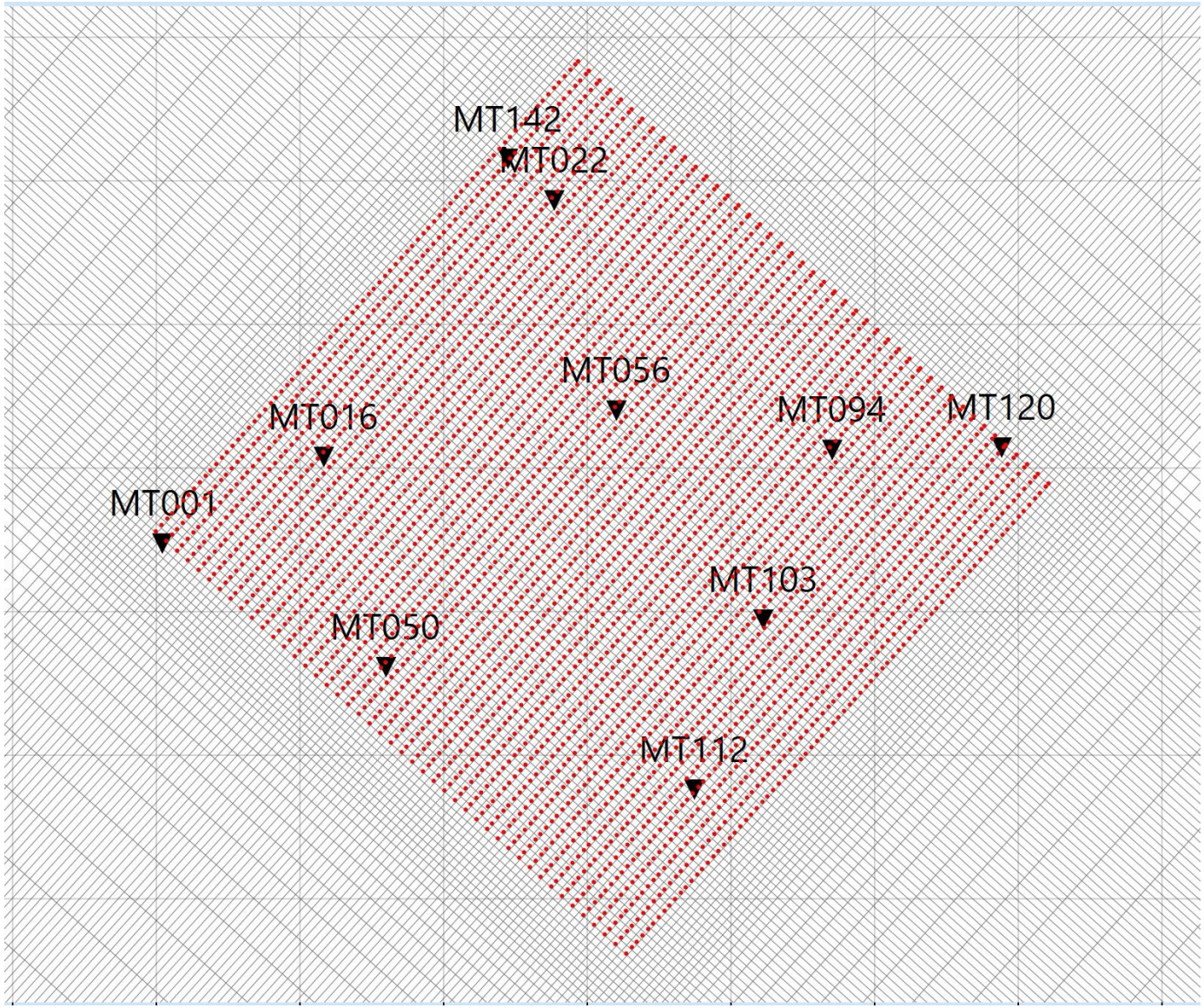

Inversion – MT+AS1

Including the MT data really aids superior imaging of the conducting zone, Rho < 30 Ωm.

After 50 iters the body is slightly below the mineralization, but that is because the AS1 data have poor depth control

Start model: 200 Ωm half-space

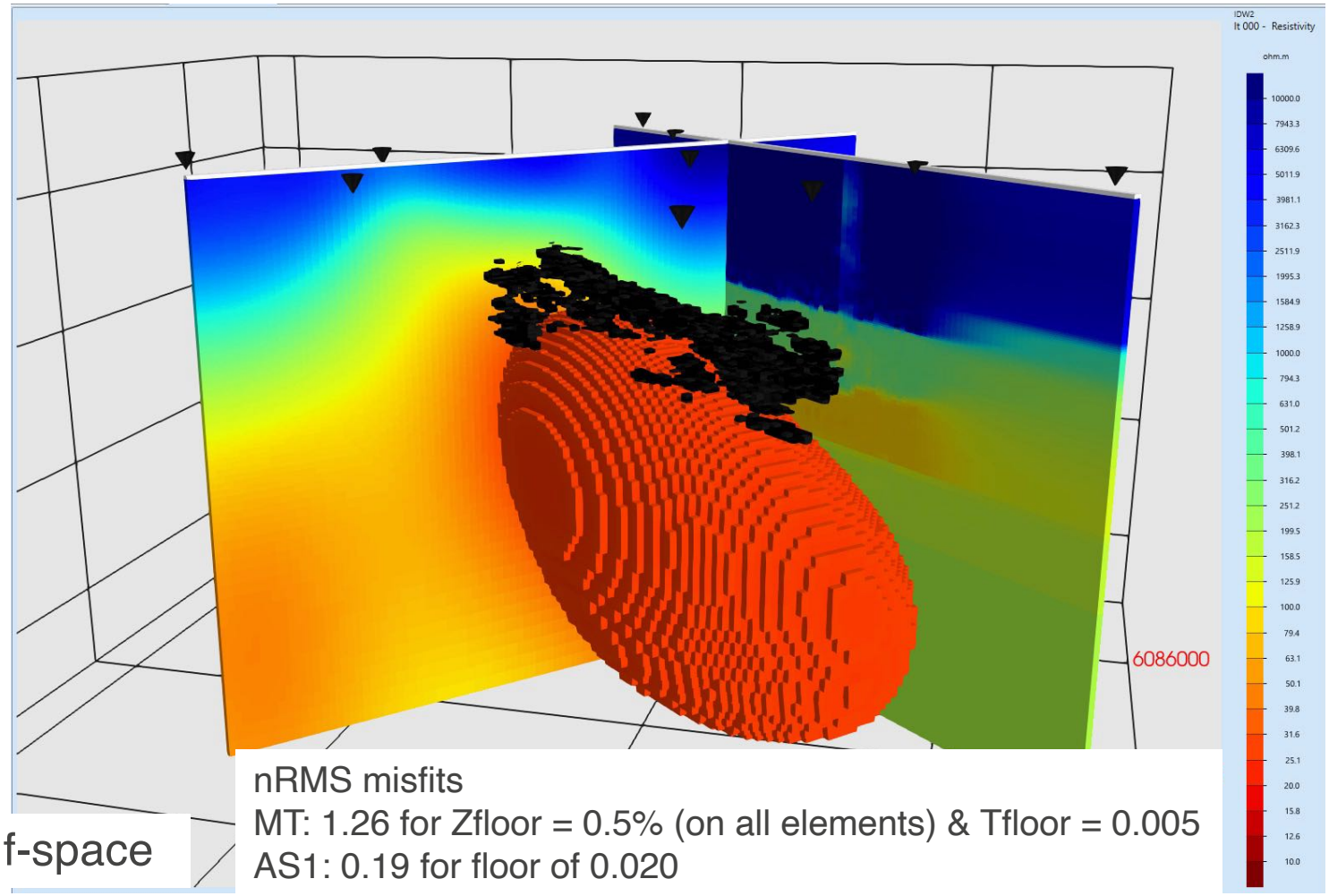

nRMS misfits
MT: 1.26 for Zfloor = 0.5% (on all elements) & Tfloor = 0.005
AS1: 0.19 for floor of 0.020

Inversion – MT+AS2

Including the MT data really aids superior imaging of the conducting zone, Rho < 30 Ωm. (Surface=100Ωm)

The core of the body is below the mineralization, but that is because the AS2 data have poor depth control

Start model: 200 Ωm half-space

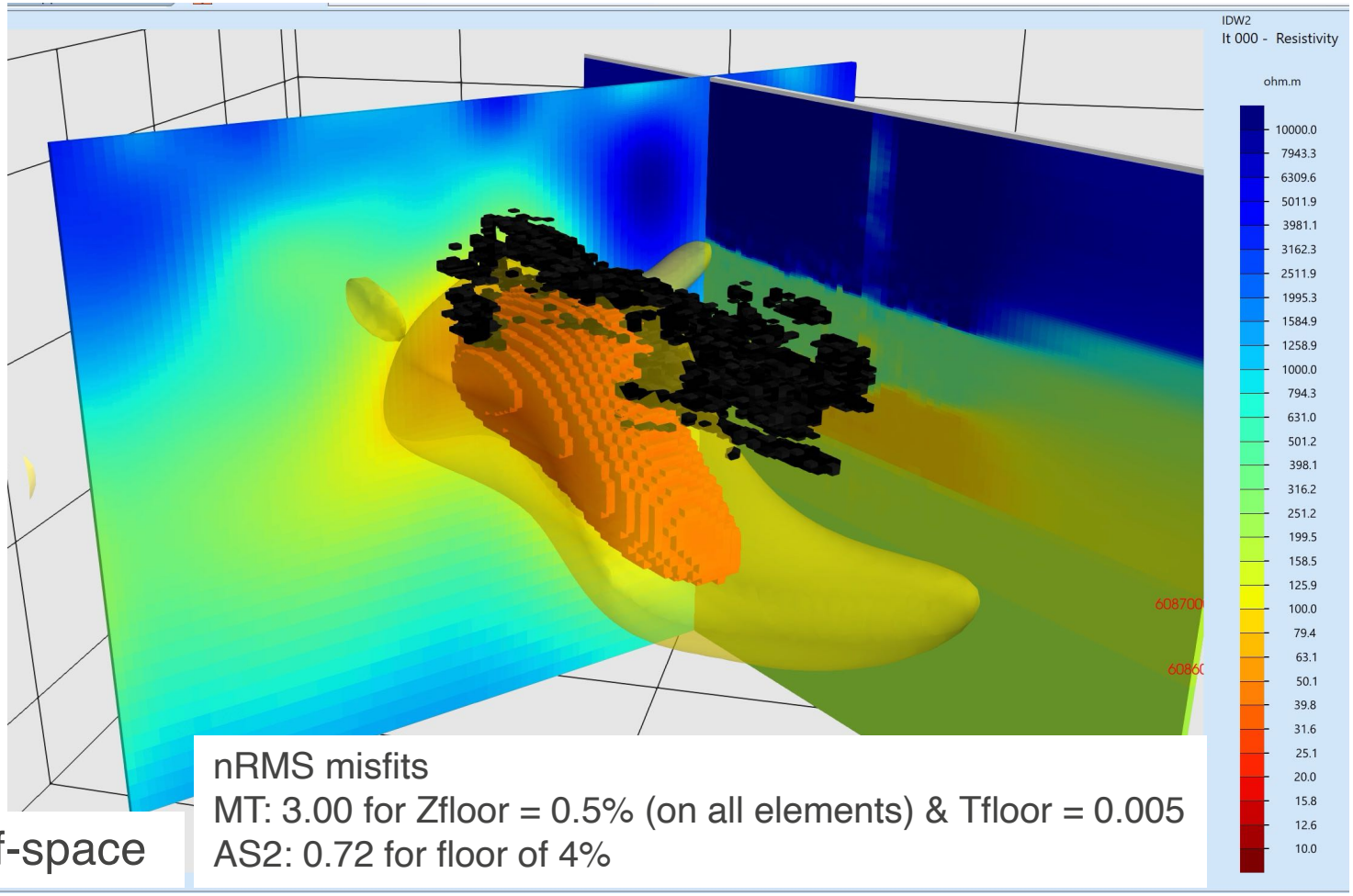

nRMS misfits
MT: 3.00 for Zfloor = 0.5% (on all elements) & Tfloor = 0.005
AS2: 0.72 for floor of 4%

Conclusions

Emphasize that some of these conclusions are for the Lalor deposit numerical model only, and generalization may not be valid

- ➔ Airborne natural source EM methods are far less sensitive to conducting deposits, but their far higher data quantity (10x – 100x) do go some way to making up for the lack of e-fields being measured. But error levels need to be significantly reduced.

- ➔ Inversion of airborne natural source EM methods aided hugely by sprinkling some MT sites within the array (same conclusion reached by Soyer et al. in 2018 AEM study)

References

Chave, A.D., and Jones, A.G., 2012. The Magnetotelluric Method, Theory and Practice, Cambridge University Press.

Larnier, H., Chubak, G., Schneider, M., Schiffler, M., and Stolz, R., 2021. Three component SQUID based system for Airborne Natural Field Electromagnetics. SEG abstract, 1290-1294.

Legault, J., Wilson, G.A., Gribenko, A.V., Zhdanov, M.S., Zhao, S., & Fisk, K., 2012. An Overview of the ZTEM and AirMt Airborne Electromagnetic Systems: A Case Study from the Nebo-Babel Ni-Cu-PGE Deposit, West Musgrave, Western Australia. Preview, 2012 (158), 26–32.

Prikhodko, A., Bagrianski, A., Wilson, R., Belyakov, S., and Esimkhanova, N., 2024, Detecting and recovering critical mineral resource systems using broadband total-field airborne natural source audio frequency magnetotellurics measurements, Geophysics, 89, WB13-WB23.